Journal of Pharmaceutical Sciences xxx (2023) xxx-xxx

Contents lists available at ScienceDirect

Journal of Pharmaceutical Sciences

journal homepage: www.jpharmsci.org

Review

Selected Aspects of the Analytical and Pharmaceutical Profiles of Nifurtimox

Q1 Aldana B. Moroni, Natalia L. Calvo, Teodoro S. Kaufman*

Área de Análisis de Medicamentos, Facultad de Ciencias Bioquímicas y Farmacéuticas, Universidad Nacional de Rosario e Instituto de Química Rosario (IQUIR, CONICET-UNR), Suipacha 531, Rosario S2002LRK, Argentina

ARTICLE INFO

Article history:
Received 23 January 2023
Revised 16 February 2023
Accepted 16 February 2023
Available online xxx

Keywords:
Analytical chemistry
BCS
Nifurtimox
Metabolism
Physical characterization

ABSTRACT

Nifurtimox is a nitroheterocyclic drug employed for treatment of trypanosomiases (Chagas disease and West African sleeping sickness); its use for certain cancers has also been assessed. Despite having been in the market for over 50 years, knowledge of nifurtimox is still fragmentary and incomplete. Relevant aspects of the chemistry and biology of nifurtimox are reviewed to summarize the current knowledge of this drug. These comprise its chemical synthesis and the preparation of some analogues, as well as its chemical degradation. Selected physical data and physicochemical properties are also listed, along with different approaches toward the analytical characterization of the drug, including electrochemical (polarography, cyclic voltammetry), spectroscopic (ultraviolet-visible, nuclear magnetic resonance, electron spin resonance), and single crystal X-ray diffractometry. The array of polarographic, ultraviolet-visible spectroscopic, and chromatographic methods available for the analytical determination of nifurtimox (in bulk drug, pharmaceutical formulations, and biological samples), are also presented and discussed, along with chiral chromatographic and electrophoretic alternatives for the separation of the enantiomers of the drug. Aspects of the drug likeliness of nifurtimox, its classification in the Biopharmaceutical Classification System, and available pharmaceutical formulations are detailed, whereas pharmacological, chemical, and biological aspects of its metabolism and disposition are discussed.

Introduction

Chagas' disease is a zoonosis caused by the protozoan parasite *Trypanosoma cruzi*. It is one of the most relevant public health problems and a major cause of morbidity and mortality among poor people in most developing countries of Latin America. Poor sanitary conditions, coupled with migrations of rural populations to urban zones have greatly contributed to the spread of the disease. Furthermore, it is beginning to be a health issue in non-endemic countries, as a result of migration waves originating in infected areas.

Within the human body, the main targets of the disease include the gastrointestinal tract and the nervous system. The evolution of the disease is divided into two well-defined phases, with a 'silent' asymptomatic stage between them; an acute phase, where the parasite can be identified in blood samples by direct examination, and a chronic phase.

The acute phase is usually acquired during childhood; it is asymptomatic, but nearly 5% of the patients develop organ damage and some die. Without treatment, the infection evolves up to the chronic phase which can be lifelong, and symptoms may appear even decades after the initial infection.[1] Nearly one-third of the infected patients display chronic chagasic cardiomyopathy,[2] characterized by mega viscera, arrhythmias, atrioventricular blockade, apical aneurysm, and ventricular dysfunction, all of which end in heart failure.[3] Stroke due to pulmonary or cerebral embolism, sudden death, and heart failure are the main causes of morbidity and mortality.[4,5]

Currently, only two drugs are available to treat this disease, and nifurtimox (Fig. 1) is one of them. The drug [Bayer 2502, (*E*)-3-methyl-4-(((5-nitrofuran-2-yl)methylene) amino)thiomorpholine 1,1-dioxide] was launched by Bayer in 1967;[6] however, 30 years later, its production was discontinued due to lack of demand, but it was soon resumed under the patronage of the WHO, as a repurposed drug for treating late-stage African trypanosomiasis, as part of the nifurtimox-eflornithine combination therapy.[7,8] The needs for Latin America were considered again in 2012.[9] Nifurtimox has been examined as a treatment for pediatric neuroblastoma[10,11] and other pediatric tumors,[12] and has also been patented as a drug to treat cancer and inhibit angiogenesis.[13]

Nifurtimox is marketed by Bayer in the form of tablets (Lampit), to be administered for 90 days (acute infection) to 120 days (chronic infection), at a level of three tablets every day. The efficacy of the

* Corresponding author.
E-mail address: kaufman@iquir-conicet.gov.ar (T.S. Kaufman).

https://doi.org/10.1016/j.xphs.2023.02.015
0022-3549/

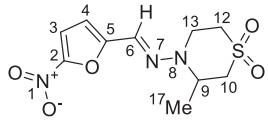

Figure 1. Chemical structure of nifurtimox. The numbering of the compound is according to Elguero et al.[14]

treatment stems from the reduction in parasitemia and antibody titers, while its expected benefit relates mainly to a reduction in the incidence of chronic complications and death. The drug exhibits many side effects and significant toxicity, such as gastrointestinal disturbances followed by neurological symptoms (neurosensory disorders, insomnia, memory disorders, and irritability),[15] which challenge patient compliance.

Nifurtimox is recommended for both, acute and chronic phases, but its efficacy has been mainly proven in terms of reducing parasitemias and antibody titers.[16] The treatment efficacy for stopping the progression of heart disease is still under debate. The expected benefits of using the drug include a reduction in the incidence of chronic complications and death.[17]

Chemical Synthesis

The synthesis of nifurtimox (**1**), which inspired the preparation of related compounds, has been reported in scientific[18] and patent[19] literature. In one of the synthetic sequences (Scheme 1), the patented diol sulfide **4**,[20] which may be obtained by the nucleophilic attack of mercaptoethanol (**2**) on propylene oxide (**3**) with subsequent epoxide ring opening,[21] is oxidized to the corresponding sulfone **5** with hydrogen peroxide under acidic conditions provided by phosphoric acid in a refluxing aqueous medium.[22] Next, the sulfone intermediate is cyclocondensed with *tert*-butoxycarbonylhydrazine or hydrazine, under basic conditions, to provide the cyclic hydrazine derivative **6**, presumably resulting from substitution at the secondary alcohol level and further dehydrative cyclization and hydrolysis of the *tert*-butoxycarbonyl moiety in the refluxing aqueous NaOH medium used for this process.

To complete the synthesis, compound **6** is condensed with 5-nitrofuran-2-carbaldehyde (nitrofurfural, **7**) in refluxing ethanol, to yield nifurtimox (**1**).[23] Nitrofurfural may be obtained by direct nitration of furfural (**8**).[24,25] In principle, the hydrazone can adopt the *syn* and *anti* (*Z* and *E*, respectively) configurations; however, only the *E*-configuration is observed in the product, presumably as a result of steric interactions between the methyl group attached to the six-member ring and the vinyl proton of the hydrazone moiety.

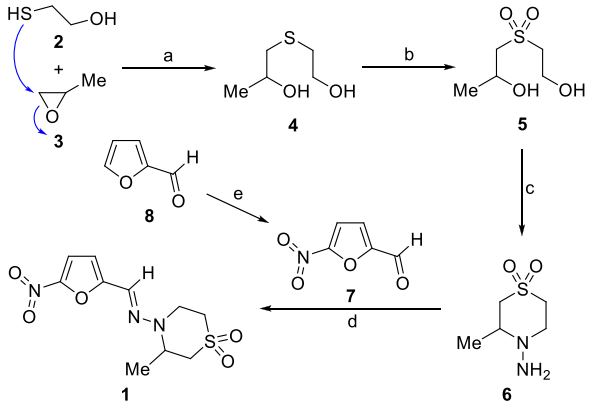

Scheme 1. *Reagents and conditions:* a) $BnMe_3N^+HO^-$, 20°C, 10 min; b) H_2O_2, H_3PO_4, reflux; c) NaOH, $^tBuOC(O)NH\text{-}NH_2$, H_2O, reflux or $H_2\text{-}NH_2$, NaOH, H_2O; d) **4**, EtOH, reflux, 24 h; e) HNO_3, H_2SO_4 (cat.), Ac_2O, 0°C, 1 h. For details on the different synthetic steps and intermediates, see refs. [18-25].

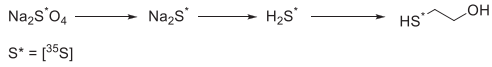

Scheme 2. Preparation of $^{[35]}$S-mercaptoethanol as a precursor for radiolabelled nifurtimox.[28]

Differently radiolabeled versions of nifurtimox have been custom synthesized and used for pharmacological studies. These included nifurtimox-d_8,[26] [^{3}H]nifurtimox[27] and [^{35}S]nifurtimox.[28] The preparation of [^{35}S]nifurtimox has been reported to proceed along these lines, using [^{35}S] mercaptoethanol as starting material. Such compound was synthesized by reduction of radiolabelled sodium sulfate ($Na_2{}^{[35]}SO_4$) to the corresponding sulfide ($Na_2{}^{[35]}S$), further liberation of the gaseous hydrogen sulfide ($H_2{}^{[35]}S$), and final hydrogen sulfide-mediated ring opening of ethylene oxide (Scheme 2).

Analogues of Nifurtimox

Following an analogous synthetic approach, differently substituted thiomorpholines and related compounds were condensed with **7**,[29] resulting in a series of analogues with general structure **9**. Fig. 2 displays some of the representative substitution patterns of the resulting analogues.[18]

Interestingly, the same condensation approach has been employed in other contexts,[30] including the preparation of other bioactive hydrazones[31] and by Enders et al.[32] for the synthesis of valuable 2-furfurylhydrazones, useful as chiral auxiliaries for the asymmetric synthesis of 3-substituted dihydro-2*H*-isoquinolin-1-ones, dihydro- and tetrahydro-isoquinolines, in moderate to good yields and high enantiomeric excesses (*ee* = 85–99%). Formic acid in benzene and even HCl have been employed as promoters, to facilitate the reaction.

Chemical Degradation

A study on the chemical degradation of nifurtimox was disclosed (Scheme 3), informing that treatment with sodium formate and nitrous oxide under neutral aqueous conditions results in furan ring opening and the formation of unsaturated nitrile **10**.[33] This complements electrolytic studies under non-aqueous conditions, using *N,N*-dimethylacetamide as the solvent, resulting in hydroxylamine derivative **11** and then in the related amine **12**.[34]

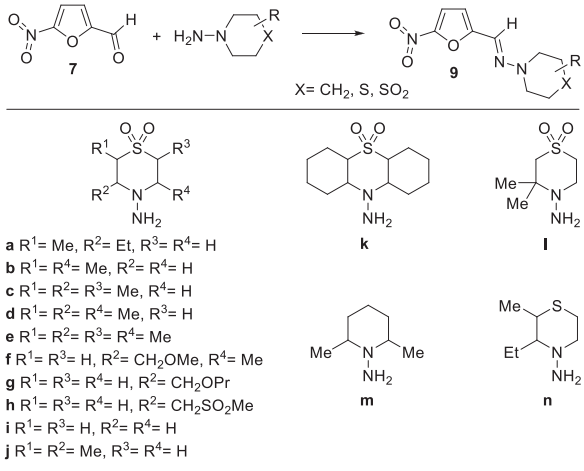

Figure 2. Substitution patterns of representative analogues of nifurtimox (**9a-n**).[18]

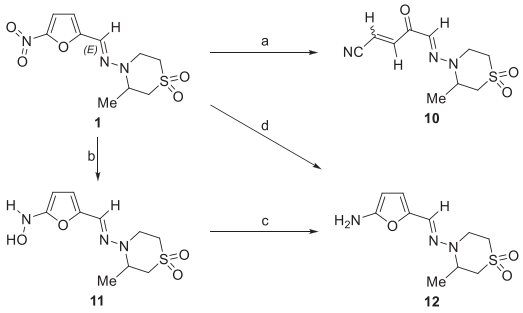

Scheme 3. *Reagents and conditions:* a) hν, HCO_2Na, N_2O, H_2O, phosphate buffer, pH 7;[33] b) electrolysis, $MeCONMe_2$, 28°C; c) electrolysis, dimethylsulfoxide (DMSO), 28°C; d) $TiCl_3$, HCl (titration).[34]

Physical Data and Physicochemical Properties

Nifurtimox (CAS Reg. N° 23256-30-6) is a yellow to orange-yellowish powdery crystalline and odorless solid, with a density of 1.483 g cm^{-3}, as determined during its crystallographic study.[14] The drug has a stereogenic centre, but it is currently marketed as a racemate, and there is unlikely to be any therapeutic benefit of a single enantiomer over the racemic mixture.[35] It has been shown that both enantiomers are equivalent in their *in vitro* activity against a panel of *T. cruzi* strains. In addition, they proved to be equivalent in their *in vivo* pharmacokinetic properties and also in their efficacy in a murine model of Chagas disease, as well as in their *in vitro* toxicity and absorption, distribution, metabolism, and excretion characteristics. The enantiomers have been separated by supercritical fluid chromatography and recrystallization, and their absolute structure was determined by X-ray diffraction.[35]

The melting point of the drug was determined as 180-182°C.[18] The lipophilicity is moderate, with a distribution coefficient of 125:1 at pH 7.4 ($\log D_{pH\ 7.4} = 2.1$).[35] Nifurtimox is a weak base at physiological pH, with a very low $pK_a = 0.34$.[36] According to the International Pharmacopeia,[37] nifurtimox is easily soluble in dimethylformamide, poorly soluble in dioxane and chloroform, and practically insoluble in diethyl ether and water. The drug has an equilibrium aqueous solubility in the range of 50-100 μg mL^{-1},[34] or even as low as 10 μg mL^{-1}[36]; its minimum solubility was estimated to take place at pH = 3.[36]

The available data regarding the logarithm of its Octanol:H_2O partition coefficient (log P) are widely divergent. This parameter has been determined under different conditions and it has been informed to be 0.04,[38] but also in the range from -0.27 to -0.25.[39,40] Other authors have determined the octanol-saline partition coefficient for [^{3}H]nifurtimox as 5.46 ± 0.03 (log P = 0.74).[27] Using [^{3}H]nifurtimox, the same group found that 6.2 ± 1.4% of the drug is bound to bovine serum albumin in artificial plasma, whereas approximately 38.9 ± 0.5% of nifurtimox was bound to albumin protein in human plasma.

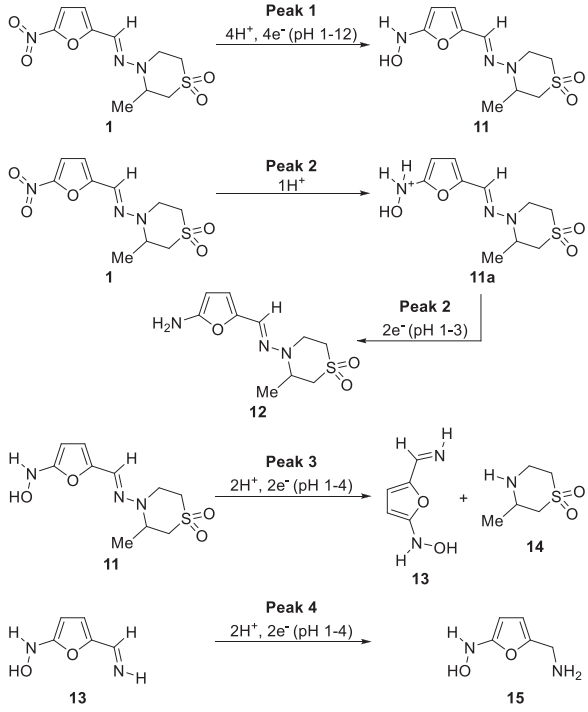

Scheme 4. Proposed mechanism for the electrochemical reduction of nifurtimox in DMF-H_2O.[34]

Analytical Characterization of Nifurtimox

Polarography

The electrochemical behavior of nifurtimox was studied in *N,N*-dimethylformamide (DMF)-H_2O,[34] at 28°C, using direct polarography with a Pt auxiliary electrode. Under acid conditions (pH 1-4) nifurtimox gives rise to four peaks; however, peaks 3 and 4 coalesce at pH 4, whereas peak 2 disappears and only two peaks are visible above pH 4. The 4-electron process of reduction of the nitro group to the related hydroxylamine **11** (Scheme 4) is the only peak observed across the whole range of pH employed (Peak 1), where the potential changed from -0.07 V at pH 2 to -0.68 V at pH 10.

The subsequent step, which entails the reduction of the protonated hydroxylamine **11a** to the related amine **12**, is a two-electron process, related to Peak 2. On the other hand, Peaks 3 and 4 represent the reductive fission of the oxime N-N bond of the hydroxylamine to afford furylimine **13** and thiomorpholine **14** and further reduction of the imine derivative **13** to the related amine **15**.

Cyclic Voltammetry

The electrochemical production and further reactions of the nitro radical anion have been the target of studies on several pharmacologically active compounds, including nifurtimox (Table 1).[41] Cyclic

Table 1
Cyclic voltammetric parameters of nifurtimox vs. saturated calomel electrode in different solvents.[a]

Solvent	E_{pc1} (mV)	E_{pa1} (mV)	ΔE (mV)	ip_a/ip_c	E_{pc2} (mV)
Citrate buffer (10^{-2} M, pH 10.5) + DMF (60:40, *v/v*)[40]	−640	−580	60	~ 990	−940
DMSO + 0.1M TBAP (scan rate: 2 V s^{-1})[44]	−900	−810	90	910	
Acetonitrile (ACN) + 0.1 M Et_4NBF_4[43]	−950	−885	65		
ACN + 0.55M H_2O[43]	−910	−835	75		−1180
H_2O[43]	−960	−895	65		−1465
DMSO[45,46]	−910	−850	60	1010	−1600
DMF[47]	−890	−840	50	830	−1300

[a] Sweep rate: 20 mV s^{-1}.

voltammetric studies of the drug indicated that the reduction mechanism depends significantly on the nature of the supporting electrolyte and solvent system used. In a protic medium (0.2 M phosphate buffer, pH 7.4), a single irreversible reduction process was observed (E_{pc} = -0.59 V), with no waves on the reverse sweep, even at a scan rate of 5 V s^{-1}. This was assigned to the reduction of the drug up to the hydroxylamine stage (R-NO_2 + $4H^+$ + 4 e^- → R-NHOH + H_2O).[42,43]

At more positive potentials, an anodic peak was observed (E_{pa} = -0.24 V), compatible with the oxidation of the hydroxylamine (R-NHOH - $2e^-$ → R-NO + $2H^+$) and confirmed by the observation of a reduction peak at E_{pc} = -0.27 V in a second sweep.

The addition of DMF or acetonitrile to an aqueous buffer modified the profile of the voltammograms. When formation of the nitro radical anion of the drug and its kinetic stability were studied in 1 mM solutions of the drug in a mixture (60:40, *v/v*) of aqueous citrate buffer (pH 10.5) and DMF, the initial irreversible four-electron reduction was observed as two separated stages. The formation of the nitro radical anion (R-NO_2 + 1 e^- → R-$NO_2^{\bullet}$) and the hydroxylamine (R-$NO_2^{\bullet}$ + $4H^+$ + 3 e^- → R-NHOH + H_2O) were clearly observed. In the case of the first stage, analysis of the CV response as a function of the scan rate (0.05-5.0 V s^{-1}) and content of DMF gave information on the stability of the radical anion. It was found that the nitro radical anion was more stable at higher concentrations of DMF and that the forward chemical decomposition reaction of the nitro radical anion follows a second-order kinetics with a stability constant of 954 M^{-1} s^{-1} and a half-life of 1.05 s.

It was also found that in a mixture (60:40, *v/v*) of 15 mM aqueous citrate buffer pH 9 and DMF, which included 0.3 M KCl and 0.1 M TBAI, nifurtimox displayed a cathodic peak potential (E_{pc} = -630 mV) for the nitro radical anion and a second order decay constant $k_2 = 0.53 \times 10^{-2}$ M^{-1} s^{-1} with a half-lifetime of 3.77 s for its decomposition.[48]

On the other hand, the E^1_7 values are parameters that account for the energy necessary to transfer the first electron to an electroactive group at pH 7 in an aqueous medium, to form a radical anion. Accordingly, pulse radiolysis data reveal that nifurtimox has an E^1_7 = -260 mV with a second order decay constant (k_2) of 1.0×10^{-6} M^{-1} s^{-1}.[49] This was in good agreement with the calculated value (E^1_7 = -257 mV) from cyclic voltammetry data. Interestingly, these results for nifurtimox could be correlated with those obtained for several analogous nitroaryl compounds and they could also be related to their biological activity against *T. cruzi*.

On the other hand, the group of Cerecetto studied the electrochemistry of 0.1 M solutions of nifurtimox and related compounds in DMSO and DMF containing TBAP (~10^{-2} M), using cyclic voltammetry three-electrode cells.[50] The latter contained a mercury dropping electrode as the working electrode, a platinum wire as the auxiliary electrode, and saturated calomel as the reference electrode.

Density functional theory calculations were performed on nifurtimox and a couple of related compounds. The studies were carried out on their neutral and radical species and used to rationalize the reduction potentials of these compounds.[51] The molecular properties determined were the energies of the Highest Occupied Molecular Orbital (E_{HOMO} = -5.72 eV), which when subtracted from the energy of the Lowest Unoccupied Molecular Orbital (E_{LUMO}) yields the energy of the gap (E_{GAP} = E_{LUMO} - E_{HOMO} = -1.73 eV). It was found that the NO_2 moiety is the more electrophilic part of the molecule and that the LUMO is localized in the NO_2 group.

The authors concluded that the electrochemical reductions occur in the nitro group because it is the most susceptible moiety to nucleophilic attack. In addition the ability of the compounds to reduce species was in agreement with their values of E_{GAP} and E_{HOMO} and with the experimental data for their *in vitro* trypanocidal activity on trypomastigotes and antriproliferative activity on epimastigotes.

Nifurtimox showed two well-defined reduction waves. The first wave corresponds to a reversible one-electron transfer, while the reverse scan displayed the anodic counterpart of the reduction waves. The breadth of the cathodic waves at their half intensity displayed a value of 55 ± 5 mV, and the intensity ratio ip_a/ip_c had a value of 920 ± 90 mV, which is typical of a pure electrochemical quasi-reversible mechanism.

According to the standard reversibility criteria, this couple corresponds to a reversible diffusion-controlled one-electron transfer without adsorption interference, attributable to the reduction of the nitro group to the corresponding stable radical anion. The second cathodic peak proved to be irreversible at all sweep rates (50-1000 mV s^{-1}) and was related to the generation of the hydroxylamine derivative.

The group of Sánchez-Urbán[43] studied the voltammetric behavior of nifurtimox in the presence of biomolecules and glutathione. In the presence of biomolecules, two reduction signals are observed in aprotic medium, corresponding to the reversible formation of the nitro radical anion and its further reduction to the hydroxylamine, by a three electrons and four protons process. The addition of glutathione (0.4 - 1.6 mM) to 1 mM nifurtimox in 0.1 M ACN-Et_4NBF_4 as electrolytic medium, did not affect the first electro-reduction wave; however, when a glassy carbon electrode (3 mm^2) was used along with a scan rate of 0.1 V s^{-1}, the second electron-transfer became strongly modified.

Summarizing, the cyclic voltammetry studies enabled to acquire a better understanding of the redox properties of the drug and its behavior in the organism, including its interaction with enzymes of the metabolism and its reduction mechanism. It also facilitated the development of electrochemical analytical methods for the determination of the drug.

Ultraviolet-Visible Spectroscopy

In water solutions, nifurtimox displays two maxima in the UV-Vis region, at about 275 nm and 400 nm (ε = 15000 L mol^{-1} cm^{-1}), and two minima at about 219 and 321 nm (Fig. 3).[34,52] Some of them, such as the first minimum and the second maximum have been selected as detection wavelengths in HPLC-based analytical methodologies for the drug.

Electron Spin Resonance Spectroscopy

ESR spectra of the electrogenerated nitro radical anion of nifurtimox were acquired at −1.2 V vs Fc^+/Fc during the study of its

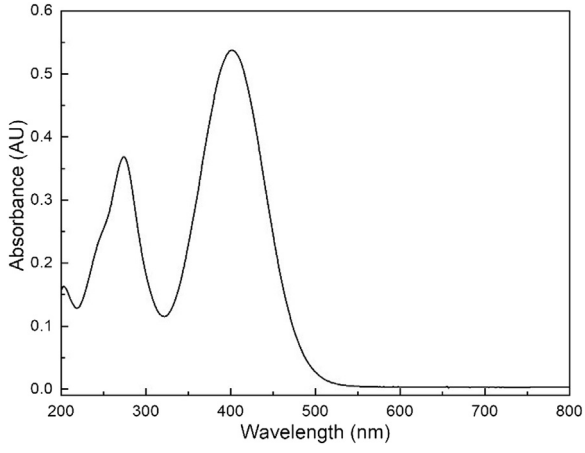

Figure 3. UV-Vis spectrum of nifurtimox in water, in the range 200-800 nm. The spectrum was taken by the authors and is in agreement with those of refs.[34,52].

Table 2
Assignment of signals of the ^{1}H, ^{13}C and 2D NMR spectra of nifurtimox in $CDCl_3$.[a]

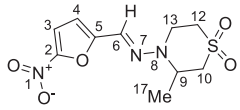

Position[b]	^{1}H NMR (δ, ppm; J, Hz)	^{13}C NMR	COSY	HMBC	HSQC
2	-	151.4	-	-	-
3	7.38, d, 1H, J = 3.6	113.9	H4	C2, C4, C5	C3
4	6.74, d, 1H, J = 3.6	108.9	H3	C2, C3, C5	C4
5	-	154.0	-	-	-
6#	7.46, s, 1H	125.0	H13	C4, C5	C6
9*	4.10, ddq, 1H, J = 6.9, 9.9 and 13.9	57.8	H10, H17	-	C9
10a	2.95, dd, 1H, J = 9.9 and 13.9	56.5	H9	C17	C10
10e	3.06, dt, 1H, J = 3.0 and 13.9				
12a	3.16, ddd, 1H, J = 3.6, 11.7 and 14.1	45.4	H13	C9	C12
12e	2.85-2.93, m, 1H				
13*	4.25, dt, 1H, J = 15.6, 3.6	43.6	H12	C12	C13
	3.79, ddd, 1H, J = 2.7, 11.7 and 15.6		H6	C9	
17	1.54, d, 3H, J = 6.9	17.7	H10, H9	C10, C9	C17

[a] Data (300 MHz) were acquired and assigned by the authors; the chemical shifts and their assignments are in agreement with those provided by Elguero et al.[14]
[b] The resonances marked with an asterisk (*) exhibit strong NOE enhancement of the signal marked as "#".

interaction with triolein, to examine the influence of molecules that mimic cellular membranes on the radical anion. The width of the signal was analyzed because this parameter is related to the electronic spin density of the radical anion and is directly proportional to the increase in the concentration of triolein in solution. The enlargement in the width of the signal suggests that nifurtimox has additional places where it shares its electronic spin density, meaning that it could be a direct interaction between the nitro radical anion and triolein.

A concomitant UV-vis analysis of the nitro radical anion - triolein system revealed that absorption bands located at 360, 500, and 550 nm, which are associated with the former component, disappeared upon the addition of 0.025 mM triolein, indicating a strong interaction between these species. The spectroelectrochemical cell included a Pt mesh (~ 0.2 cm^2) working electrode, a Pt wire (2.5 cm^2) as the counter electrode, and a Ag/Ag^+ (0.01 M $AgNO_3$ + 0.1 M TBAP in ACN) reference electrode.

Nuclear Magnetic Resonance Spectroscopy

Elguero et al. published the NMR chemical shift data of nifurtimox in $CDCl_3$ (Table 2). The more recent addition of 2D spectra (COSY, HMBC and HSQC) provided additional insights and an unequivocal assignment of all signals. On the other hand, Holtzer used nuclear Overhauser effect (NOE) data to confirm the stereochemistry of the drug in solution.[53] The *E*-configuration was unambiguously assigned based on the observation of a strong NOE enhancement on the singlet signal of the iminyl-CH moiety (N=C*H*) upon irradiation of the multiplets assigned to NCH_2 and NCH of the thiomorpholine moiety.

The absence of long-range proton-proton couplings of H4 (^{4}J) and H3 (^{5}J) with H6 suggested that their solution conformation is *s-cis*, consistent with that of furfural in polar solvents such as DMSO.[54,55]

Single Crystal X-Ray Diffractometry

The group of Elguero reported the X-ray diffraction data of nifurtimox, acquired using CuK_α radiation (λ = 1.54188 Å).[14] They informed that the crystal phase has two crystallographically independent molecules, with slightly different bond lengths and bond angles (Cambridge Crystallographic Data Centre deposition N° 1182040; database identifier: JAHPEN). Both molecules are present in an *s-trans* conformation about C5-C6, which has a bond length of 1.44 Å and some double bond character due to resonance (Scheme 5).

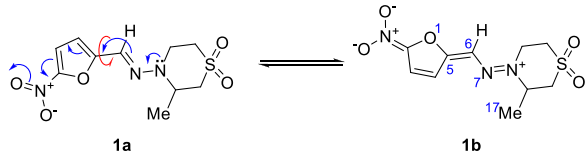

1a **1b**

Scheme 5. Some resonance forms of nifurtimox.[14]

The resonant forms **1a↔1b** explain the observed planarity of nifurtimox, resulting from dihedral angles O1-C5-C6-N7 of 184.2 and 180.9° for both conformers of the unit cell. Because the barriers to *syn/anti* isomerization in hydrazones are too high, it can be anticipated that solutions of nifurtimox will keep the *s-trans* configuration, as confirmed by NMR analysis.

On the other hand, the diffraction data confirmed that the methyl group is equatorial and that the thiazine ring takes a chair-like shape. Additional characteristics of the crystal phase are shown in Table 3. To date, except for the very recent characterization of an amorphous phase,[56] no other solid-state forms of the drug (including structural polymorphs and solvates) have been reported. The latter publication contains detailed analyses of the spectroscopic (solid-state NMR, mid and near-infrared) and thermal (differential scanning calorimetry, thermogravimetry) characteristics of the crystalline and amorphous phases, along with hot stage microscopy, powder X-ray diffractometry, and functional (solubility, dissolution) information.

Analytical Determination of Nifurtimox

Polarography

The development of polarographic methods for the determination of nifurtimox was based on the redox properties of the nitro moiety attached to the furan ring. Chronologically, the reports of these methods preceded the development of simpler spectrophotometric alternatives. As part of their study on the drug, Squella et al. developed a polarographic method for the determination of nifurtimox in synthetic samples and commercial tablets. The recovery rates were 99.2 ± 1.8% and 99.6 ± 1.9%, respectively.[57]

In vivo, nitrofuran derivatives are generally metabolized to their corresponding amines via nitroso and hydroxylamine intermediates. However, in the polarographic experiment, the reduction of the nitroso group to hydroxylamine occurs at a more positive potential than the reduction of the nitro group, so the reduction is not detected. This polarographic method could be used in metabolic

Table 3
Crystal parameters of nifurtimox at room temperature, as informed by Elguero et al.[14]

Parameter (units)	Value	Parameter (units)	Value
Chemical formula	$C_{10}H_{13}N_3O_2S$	Crystal dimensions (mm)	0.27/0.27/0.30
Formula weigth	287.29	α (°)	92.890(4)
Crystal color	Yellow	β (°)	104.974(3)
Space group	$P\bar{1}$	γ (°)	80.1 85(4)
a (Å)	11.491 5(5)	V (Å^3)	1286.3(1)
b (Å)	13.191 9(6)	δ calc. (g cm^{-3})	1.483
c (Å)	8.9143(3)	μ (cm^{-1})	24.07

Table 4
Colorimetric methods for the determination of nifurtimox.[a]

Method Parameter Substrate	A Nifurtimox	B Nifurtimox	C Nifurtimox	D Reduction product	E Hydrolysis product	F Nifurtimox	G Nifurtimox
Color reagent system	Direct Spectro-photometry	Direct Spectro-photometry	Direct Spectro-photometry	3-Methyl-2-benzothiazolinone hydrazone $FeCl_3$	2-Thiobarbituric acid	NBS, Metol - isonicotinic acid hydrazide	Chloramine T Gallocyanine
Sample type	Urine	Plasma, Organs	Plasma	Drug formulations	Drug formulations	Drug formulations	Drug formulations
Range (μg mL^{-1})	0.5-10	1-20	1.77-10 (LOQ = 1.77)	2.5-10	2.5-30	1.25-7.5	0.8-5.6
Recovery (%)	~80	90	92.8-96.8	99.2-100.9	99.2-100.9	99.2-100.9	99.8-102.1
$E \times 10^3$ (L mol^{-1} cm^{-1})		0.58		8.5	5.86	21.8	21.55
Sandell's sensitivity (μg cm^2 10^3 AU)				0.033	0.049	0.013	
RSD (%)			4.14 (n = 21)	0.72 (n = 6)	0.29 (n = 6)	0.84 (n = 6)	0.87 (n = 6)
Wavelength (nm)	400	400	400	620	530	620	540
Waiting period (min)	0	0	0	< 5	< 60	5-20	25-40

[a] For details of the different methods, see refs. [58] (Methods A and B), 59 (Method C), 60 (Methods D-F) and 69 (Method G).

studies as a means to monitor the hydroxylamine intermediate simultaneously with the parent compound.

Differential pulse polarograms acquired at 6.0 demonstrated method specificity and selectivity, separating the nitro peak (selected for quantitative studies) from the azomethine peak. The peak current is linearly dependent on the temperature (0.38°C^{-1}), with the square root of the mercury height column and the nifurtimox concentration (range 10^{-7}–10^{-4} M), in agreement with a diffusion-controlled process.

Spectroscopic Methods in the UV-Vis Region

Medenwald et al. developed the first direct spectrophotometric method (Table 4, Method A) for the determination of nifurtimox, using urine samples.[58] The procedure entailed the extraction of the sample with toluene, followed by evaporation of the organic solvent, redissolution of the residue in acetone, and finally a spectrophotometric determination at 400 nm. The valid linear range is 0.5-10 μg mL^{-1}, where drug recovery is ~80% and absorbance readings resulting from a 5 μg mL^{-1} solution are ~0.75.

The same group reported an alternative method for plasma samples (Method B), where MeOH was employed for deproteination, and after evaporating the solvent, the residue was dissolved in acetone and passed through a silica gel column, eluting with acetone. The absorbance of a concentrated sample of the eluate was determined at 400 nm and the concentration of the drug was obtained by interpolation of a calibration curve. The sensitivity of the method was determined to be 0.5 μg mL^{-1} and drug recovery was 90%. The apparent $E_{1\%,1cm}$ was 580 and the method proved to be useful for plasma concentrations of nifurtimox in the range of 1-20 μg mL^{-1}. The method can also be used for organ samples (liver, kidneys, spleen, and brain), despite the higher blanks and lower sensitivity. However, one of its drawbacks is that the silica gel column and the calibration curve can only be used once.

The group of Bulffer developed and validated an alternative direct spectrophotometric method[59] for the determination of nifurtimox and benznidazole in plasma samples (Table 4). During the procedure (Method C), the organics were extracted by passage through an Extrelut column. The extract was evaporated and the residue was redissolved in MeOH:H_2O; finally, its absorbance was recorded at 400 nm, and the results were compared against a standard solution of the drug. This method was applied to plasma samples obtained from rats, to which a high dose of the drug was administered. The method requires 1 mL of blood and some of the validation parameters, such as accuracy, precision, and limit of quantification, are less satisfactory than the indirect spectrophotometric methods based on the generation of alternative chromophores.

Sastry et al. reported four simple and sensitive spectrophotometric methods for the determination of nifurtimox, suitable for their application on bulk drug and tablet formulations.[60] One of these approaches (Method D) is based on the formation of a colored species when the furfurylamine derivative **12** (Scheme 6) is treated with the 3-methyl-2-benzothiazolinone hydrazone (MBTH, **16**)/ferric chloride reagent system.[61]

In this process, based on the method described by Sawicki,[62,63] MBTH is oxidized to the related charged **17** and **17a** (resonant species), which in turn can participate in an electrophilic aromatic substitution on the electron-rich furan ring of **12** to give the colored product **18**. The reduced species **12** is conveniently obtained by a Zinc/HCl-mediated reduction of the active pharmaceutical ingredient (API).

In a second alternative (Method E),[60] nifurtimox is hydrolyzed under acidic conditions to furnish the aldehyde **7** and the substituted

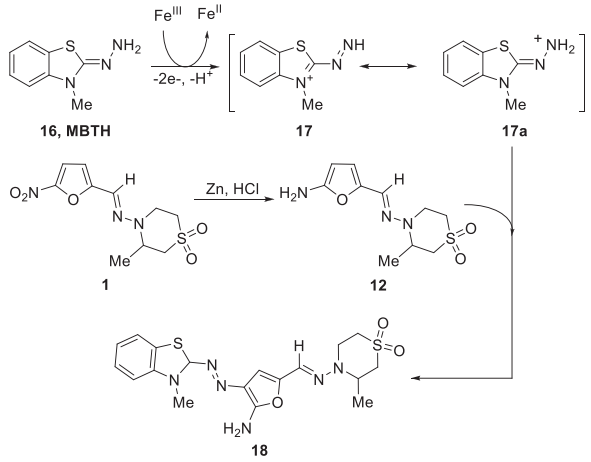

Scheme 6. Colorimetric determination of nifurtimox under oxidizing conditions. Reaction with MBTH (**16**) and Fe(III).[60,61]

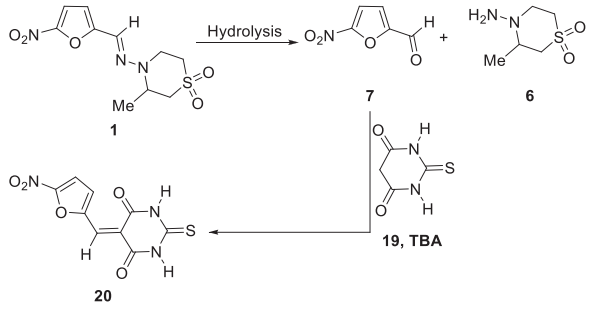

Scheme 7. Colorimetric determination of nifurtimox by hydrolysis and reaction of the resulting 5-nitro-2-furfuraldehyde **7** with thiobarbituric acid (**19**).[60,64-66]

hydrazine **6**,[64,65] which upon exposure to 2-thiobarbituric acid (TBA, **19**) in an HCl-AcOH-H_2O medium affords the colored species **20** (Scheme 7).[66] The latter is determined at 530 nm (ε = 5860 L mol^{-1} cm^{-1}).

On the other hand, the third method (Method F)[60] entails a two-stage scheme where the API is first made to react with excess *N*-bromosuccinimide (NBS, **21**), resulting in succinimide (**22**) which does not interfere. Then, the remainder of the oxidant is reduced with metol (**23**), which becomes converted into the related quinone-imine (PMBQMI) **24** (Scheme 8). In turn, the latter is exposed to isonicotinic acid hydrazide (INH, **25**), affording the colored complex **26**, which is

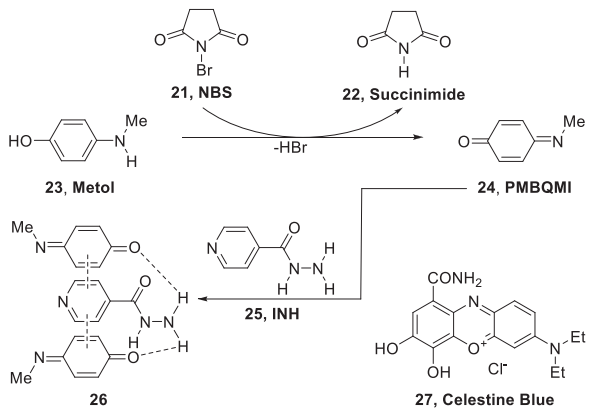

Scheme 8. Colorimetric determination of nifurtimox. Chemical basis of the quantitation of excess NBS (**21**), through the reaction with metol (**23**) and complexation of the resulting oxidation product (PMBQMI, **24**) with INH (**25**). The excess of NBS can also be determined with the Celestine Blue dye.[67,68]

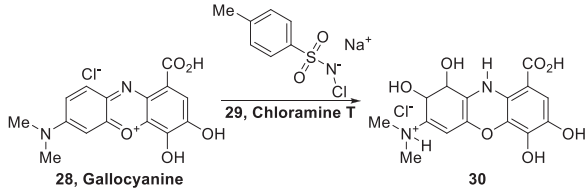

Scheme 9. Quantitation of nifurtimox with Chloramine T (**29**) as oxidant. Determination of the excess of oxidant with Gallocyanine (**28**).[69]

determined at 620 nm (ε = 21800 L mol^{-1} cm^{-1}). Most probably π-stacking between the quinone ring systems and the pyridine moiety takes place, favored by hydrogen bonding, whereas the generation of a charge transfer complex contributes to the color.[67] The method requires close control of the pH and the so-formed charge-transfer complex is slightly unstable.

An alternative procedure involves the addition of a known excess of NBS to the sample, in the presence of 0.25M HCl and the determination of the unreacted NBS by measuring the decrease in the absorbance of the dye Celestine Blue (**27**), at λ_{max} = 540 nm (ε = 108000 L mol^{-1} cm^{-1}).[68] The method is useful for pharmaceutical formulations. It was found that time spans of 5-20 min for the first reaction and 2-30 min for the second stage gives the best sensitivity (Sandell's sensitivity = 2.67 × 10^{-3} μg cm^2 10^3 AU).

The method was applied for the the drug content determination test in pharmaceutical formulations at the microgram level (0.2-5 μg mL^{-1}), with low standard deviations (RSD = 0.17%, n = 6) and high recoveries (99.8-101.1%). These methods were free from interferences of the tablet matrix, including excipients such as starch, lactose, talc and magnesium stearate.

The fourth indirect photometric method developed by the same group (Method G)[69] involves the addition to the sample of excess chloramine T (**29**) as an oxidant (Scheme 9), in the presence of 0.25M HCl, and the determination of the unreacted oxidant by measuring the decrease in the absorbance of Gallocyanine (**28**) at 540 nm. The dye undergoes bleaching in the presence of the HClO generated from the Chloramine T, since this reactive halogen compound may cause ring oxidation to a colorless species, such as **30**.

Chromatographic Methods

Medenwald et al. reported a bidimensional TLC method for the determination of the drug[58] in body fluids (serum, urine). Preparation of the samples involves extraction with EtOAc followed by solvent evaporation, partition of the residue between ligroin and acetonitrile and final partition of the acetonitrile phase residue between water and benzene. The residue of the benzene phase was then dissolved in MeOH and applied to a TLC plate.

The samples were eluted with $CHCl_3$ (R_f = 0.3-0.4) in the first dimension, whereas EtOAc (R_f = 0.7-0.8) was employed for the second dimension. Nifurtimox is recognized by its yellow color. Co-chromatography with a standard of the drug was employed for its unequivocal identification. For quantitation purposes, the spot containing nifurtimox was scratched off the plate and taken in DMF-pyridine; the silica gel was separated by centrifugation, and the content of the drug was determined spectrophotometrically at 410 nm.

The method is rather laborious and requires 10 mL plasma samples, which are extracted with a total of 40 mL EtOAc; it is useful in the range of 0.5-10 μg mL^{-1} with LOD = 0.1-0.2 μg mL^{-1} and has a drug recovery of 80% for standard additions in the range of 5-50 μg mL^{-1}. The apparent $E_{1\%,1cm}$ was 600. The authors reported that the addition of a drop of 2% KOEt in EtOH to the DMF-pyridine solution yielded an intense but unstable blue color (λ_{max}= 605 nm, $E_{1\%,1cm}$ = 600), which is less satisfactory for quantitative determinations.

Table 5
HPLC-based analytical determination of nifurtimox in biological samples.[a]

Parameter/Method	A	B	C	D	E
Internal standard	Nitrofurazone 30 μg mL^{-1} in H_2O	Carbamazepine 250 μg mL^{-1} in DMSO	-	-	Nifurtimox-d_8
Column	PBondapak	RP-18	ODS Hypersil	Eclipse	Luna C8(2)
Part. Size (μm)	Cl8	5	5	XDB-C18	5
ID × l (mm)	10 3.9 × 150	4.6 × 125	2.1 × 200	5 4.6 × 250	2 × 50
Mobile phase	MeOH-phosphate buffer pH 7.0 (50:50, *v/v*)	MeOH-phosphate buffer pH 7.0 (50:50, *v/v*)	400 nm: MeOH:H_2O (60:40, *v/v*) 215 nm: 25 mM KH_2PO_4 (pH 2.5)	MeOH-25 mM phosphate buffer pH 2.7 (58:42, *v/v*)	A: 2 mM NH_4OAc buffer, (pH 3 with HCO_2H) B: MeOH
Mode	Isocratic	Isocratic	Isocratic	Isocratic	Gradient %B (min): 10% (0.5) 70% (0.6-2.7) 90% (2.8-3.7) re-equilibration 10% (3.8-5.5)
Detector wavelength (nm)	400	270	400 215	395	Standard triple quadrupole tandem mass spectrometer
t_r/t_r of IS (min)	2/3	2.8/6.2	3.75	5.4/-	3.5/3.5
LOD/LOQ (ng mL^{-1})	77.0/-			15.7/47.2	10
Sample	Plasma		Tissue (cytosol), urine	Plasma	Plasma (dog)
Loop volume or sample size (μL)			1	5	50
Reproducibility (CV, %)	Intraday: 3.5 (n= 10) at 0.500 μg mL^{-1} Interday: 4 (n= 10)	5% at 15 μg mL^{-1}		Intraday: 0.76-1.79 Interday: 1.02-2.13 at 5-10 μg mL^{-1}	Intraday: 1.3-9.5 Interday: 2.6-10.1 at 0.01-10 μg mL^{-1}
Accuracy, Bias (%)				-1.4 - -2.3	+6 - +13
Recovery (%)	90.6			96.8-98.1	98.4-101
Selectivity	No plasma peaks as interferents				Negligible
Linear range (μg mL^{-1})	0.077-2.3			0.078–0.91	0.01-5
Flow rate (mL min^{-1})	1.0		0.2	1.0	0.4

[a] For details of the methods, see Refs. [70] (Method A), [26] (Method B), [73] (Method C), [74] (Method D) and [71] (Method E).

Paulos et al. disclosed the first convenient and sensitive approach for the chromatographic analysis of nifurtimox in human serum samples using RP-HPLC and UV detection (Table 5). In their approach (Method A),[70] the deproteinization was performed by precipitation with $HClO_4$, followed by separation of the liquid phase and addition of NaOH. Then, nifurtimox and nitrofurazone (internal standard) were extracted with CH_2Cl_2, the organic phase was concentrated, and after solvent exchange, the HPLC analysis was carried out. Other methods use carbamazepine (Method B) and nifurtimox-d_8 (Method E) as internal standards.

In the latter case, the stable isotope dilution technique was used, a triple quadrupole tandem mass spectrometer was employed as detector [Nifurtimox (*m/z*): parent ion (Q1) 288.3; product (Q3): 148.0; Nifurtimox-d_8 (*m/z*): parent ion (Q1) 296.3; product (Q3): 156.2;] and elution was in the gradient mode.[71] This HPLC/MS/MS method enabled the sensitive determination of nifurtimox down to 0.010 μg mL^{-1} in deproteinized plasma samples in a concentration range 0.01-5.0 μg mL^{-1}, with great interassay accuracy (Recovery = 98.4-101%) and precision (CV = 2.61-10.1%).

A useful method which does not use an internal standard has been reported by the group of Castro[72] and it was further improved (Method C) to detect the unchanged drug excreted in urine along with two more polar metabolites which the authors were unable to identify. A variation of these methods was reported for the determination of the distribution of nifurtimox across the healthy and trypanosome-infected murine blood-brain and blood-cerebrospinal fluid barriers with radioactivity detection.[27]

The method was applied to blood and brain membrane homogenates. To this end, a 100-μL aliquot of the sample containing [^{3}H] nifurtimox was injected into a 4.1 × 250 mm PRP-X300 column (7 μm) and eluted with MeOH:H_2O (60:40, *v/v*) at a flow rate of 0.3 mL min^{-1}. The column eluent was mixed with a scintillation fluid (1:3 *v/v*) in a radioactive detector, to perform real-time radioactivity analysis.

Method D, which does not require an internal standard, involves an alternative sample preparation process, based on an ionic liquid dispersive liquid-liquid microextraction (DLLME) with 1-octyl- 3-methylimidazolium hexafluorphosphate as ionic liquid in MeOH as disperser and KCl as salt.[70] Due to the presence of matrix effects, the uncommon standard addition approach had to be used for quantification. Improvements in the sample preparation were also disclosed, and the method was extended to milk samples.[75,76] Under the optimum working conditions, the average recovery was 89.7%, the LOD was 0.09 μg/mL and the inter-day reproducibility was 5.77%. The proposed methodology was considered sensitive, simple, robust, accurate, and green.

Chiral Separations

Chromatographic Methodologies

The enantiomers of nifurtimox have been separated by supercritical fluid chromatography[35] and the group of Chankvetadze performed analytical separations of different drugs, including nifurtimox, employing chromatographic (Tables 6 and 7) and

Table 6
Chiral HPLC separation of the enantiomers of nifurtimox bulk drug employing different columns and mobile phases.[77]

Column	Mobile phase	k'_1	k'_2	α	R_s
Chiralcel-OJ Cellulose (tris 4-methylbenzoate)	MeOH	1.53	2.25	1.57	1.0
Chiralcel-OD Cellulose tris(3,5-dimethylphenyl carbamate)	MeOH	0.68	0.74	1.08	-
Chiralpak-AD Amylose tris(3,5-dimethylphenyl carbamate)	MeOH	3.35	4.09	1.22	1.5
Chiralpak-AD	ACN	0.10	0.22	2.20	1.2
CDCPC Cellulose tris(3,5-dichlorophenyl carbamate)	MeOH	1.21	1.21	1.00	1.0

Table 7
Enantioseparation of nifurtimox bulk drug using Chiralcel OD[a] coated on silica gel.[78]

Mode[b]	Amount of chiral selector (% *w/w*)	k'_1	α	N_1	N_2	R_s
CLC	2	-	1.00	3404	3404	-
	5	0.07	2.02	10233	10285	1.58
	10	0.13	2.03	9153	8535	2.69
	20	0.25	1.90	10909	11158	5.62
CEC	2	0.02	1.72	22673	22977	0.62
	5	0.06	2.13	27636	31001	2.47
	10	0.19	1.68	32317	28623	4.60
	20	0.31	1.70	20876	20 45	4.10

[a] Chiralcel OD is cellulose tris(3,5-dimethylphenylcarbamate).
[b] CLC: Capillary liquid chromatography; CEC: nonaqueous capillary electrochromatography (CEC).

electrophoretic methods (Table 7). The enantiomers of nifurtimox have been submitted to chiral HPLC with different columns, Chankvetadze et al. reported the use of 250 × 4.6 mm Chiralcel-OJ, Chiralcel-OD, and Chiralpak-AD columns, in the polar organic mode, using MeOH or acetonitrile as mobile phases. Pure polar organic eluents offer some advantages, including alternative chiral recognition mechanisms, higher solubility of some analytes, low cost, and ease of removal. The runs were performed at a flow rate of 1 mL min^{-1} and detection of the analytes was performed at 254 nm.[77]

In comparison with the phenylcarbamate derivatives of polysaccharides, the phenylester type column was less efficient when pure MeOH was used as the mobile phase. The separation factors of nifurtimox were rather high but low peak efficiency did not enable the observation of a baseline enantioseparation. No baseline separation was achieved with the Chiralcel OD column either, although MeOH appeared to perform better than acetonitrile. The Chiralpak-AD column, which contains the same phenylcarbamate moiety as Chiralcel-OD but attached to an amylose backbone, exhibited a rather high enantiomer resolving ability compared to its cellulosic analogue, with MeOH as the most discriminating solvent.

Electrophoretic Methodologies

In the case of the electrophoretic methodologies (Table 7), enantioseparations employing nonaqueous capillary liquid chromatography and capillary electrochromatography using cellulose tris(3,5-dimethylphenylcarbamate) as chiral stationary phase (Chiralcel OD) were reported.[78] The effects of chiral selector loading on the silica gel, the particle size of the latter, the nature of the organic solvent, and the electrolyte salts on the separation characteristics were investigated.

It was found that the chiral selector loading onto silica gel is very significant for the enantioseparation characteristics, affecting the number of theoretical plates, as well as the resolution between peaks, their retention factors, and selectivity. It was also detected a decreasing EOF when the particle diameter was increased from 5 to 12 μm, that alcohols (EtOH and MeOH) and ACN are suitable non-aqueous solvents and that the plate numbers observed in methanol-Tris and methanol-ammonium acetate were comparable to each other.

In addition, it was observed that CEC had significant advantages over CLC, including better tolerance to higher linear flow rates and a higher plate number at similar linear flow rates of the mobile phase.

Drug Likeliness of Nifurtimox

After observing that most orally administered drugs are active if they are small molecules of moderate lipophilicity, Lipinsky proposed his seminal “rule of five”, to measure drug likeliness of a compound for oral delivery, indicating that to be active a drug should have a molecular mass below 500 daltons, a log P below 5, and be able to form hydrogen bonds through no more than five hydrogen bond donors (N-H, O-H) and no more than 10 hydrogen bond acceptors (N and O).[79] Nifurtimox complies with all four criteria: it has a molecular weight of 287.30, whereas its log P was determined as 0.04[38] and calculated (clog P) as 1.173;[80] furthermore, it has 4 hydrogen bond acceptors, and no hydrogen bond donors.

On the other hand, Veber et al.[81] also studied the oral druggable space, by examining the molecular properties that influence the oral bioavailability of drug candidates. They observed that for proper oral bioavailability, the compounds must have no more than 10 rotatable bonds and a polar surface area below 140 $Å^2$. Nifurtimox complies with both criteria; its polar surface area is 117 $Å^2$ and it has only three rotatable bonds.

The monograph of Nifurtimox in the International Pharmacopeia

The International Pharmacopeia is the only widely known compendium that carries a nifurtimox monograph.[37,82] The latter specifies identity and purity tests, as well as an assay. Accordingly, the identity of the drug can be determined by examining its mid-infrared spectrum against a spectrum of the reference substance or a reference spectrum. Alternatively, it should comply with several tests. One of these includes a color reaction test based on the complexation reaction with $CuSO_4$/pyridine in DMF-H_2O; this should afford a dark green color, which remains in the aqueous phase when the reaction mixture is diluted with $CHCl_3$. Additionally, the drug should pass a classical silica gel TLC-based identity test against a standard of the drug. The mobile phase is an EtOAc:hexane solvent mixture (1:1, *v/v*), and the spots are detected by exposure of the plate to short-wavelength UV-light (254 nm).

The purity tests include the determinations of the melting point (176-178°C), sulfated ashes (limit: 0.1%) and loss drying (limit: 0.5% after drying at 105°C until constant weight), along with a TLC run. In the latter, the limit of individual impurities is set to 2%, specifying that any secondary spot generated from the sample should not be

more intense than the principal spot originated from a suitably diluted sample. The TLC-plate of the purity test should also be used for identification; to that end, a third lane containing the standard of the drug is included in the run.

Finally, the assay consists in a classical titanometry, where the sample dissolved in a dimethylformamide:ethanol (4:1, *v/v*) mixture, is acidified with HCl and exposed to excess standardized $TiCl_3$ (Eq. 1), back-titrating the excess of titrant with a standardized solution of Mohr's salt [$FeNH_4(SO_4)_2$]. The latter becomes reduced to ferrous ion (Eq. 2), and potassium thiocyanate (KSCN), which is capable of forming a deep red complex with Fe(III) species (Eq. 3),[83] was employed as the color indicator.

$$R-NO_2 + 6TiCl_3 + 6HCl \rightarrow 6TiCl_4 + RNH_2 + 2H_2O \quad (1)$$

$$TiCl_3 + FeNH_4(SO_4)_2 \rightarrow TiCl_4 + FeSO_4 + (NH_4)_2SO_4 \quad (2)$$

$$Fe^{+3} + nSCN^- \rightarrow Fe(H_2O)_{6-}n(SCN)_n^{+3-}n \quad (3)$$

Under the titration conditions, the nitro group of the drug becomes reduced to the corresponding amino moiety,[84] with concomitant oxidation of the titanous species to Ti(IV), which remains stable under the strong acidic medium provided by hydrochloric acid. Nifurtimox is a hydrazone, which can be hydrolyzed under aqueous acidic conditions to unveil its components, the aldehyde **7** and the hydrazine **6**. Interestingly, despite it has been reported that $TiCl_3$ is capable of reacting with certain hydrazines, under the specified titration conditions this is not an interference.

Nifurtimox and the Biopharmaceutical Classification System (BCS)

The BCS approach was introduced[85] as a new paradigm in bioequivalence, based on scientific principles.[86] The system classifies the APIs according to their solubility and permeability. Class I comprises those with high solubility and permeability, whereas Class IV groups APIs with low solubility and permeability. Class II is for compounds with low solubility and high permeability, while Class III collects all APIs with high solubility and low permeability. BCS avoids costly and unnecessary human experiments, and strongly reduces the costs of developing generic products. One of its benefits is that under specific conditions, products can be approved on the bases of pharmaceutical dissolution data instead of bioequivalence studies in humans.

Drug permeability is often considered as if drugs cross biological membranes by passive transcellular diffusion, based on the relationship between log P and human intestinal permeability, using metoprolol (absorbed up to 95%) as the reference compound.[36] In this context, drugs with log P > 1.76 is classified as having high-permeability.[87] Following oral administration, nifurtimox is well absorbed, and the drug reaches plasma levels in the range of 10-20 mM; lower concentrations can be found in tissues and urine. The patient's age and disease phase are key factors in establishing a proper therapeutic schedule.[88–91]

Employing [^{3}H]nifurtimox (1.25–6 μM), it has been shown that the drug can cross the blood-brain and blood-cerebrospinal fluid barriers readily and that after 30 min of perfusion it is able to attain relevant concentrations in the frontal cortex (6.0 μM) and CSF (12 μM) which could be effective against *T. brucei gambiense* (IC_{50} 1.7 μM) and *T. b. rhodesiense* (IC_{50} 1.5 μM).[27]

The solubility of nifurtimox is consistent with the characteristic of a practically insoluble drug;[92] However, as manifestation of the poor knowledge of the drug, some authors have considered its aqueous solubility at notably higher values, ranging from the calculated 1.44 mg mL^{-1},[93] to 2.39 mg mL^{-1},[38] and even up to 33 mg mL^{-1}.[94]

According to different authors, and probably due to the lack of proper knowledge of the properties of the drug, nifurtimox was placed in different BCS classes, including Class II,[95,96] (especially at lower doses),[36] Class III[97–101] and Class IV. The placement of nifurtimox in Class III was a result of the poor knowledge of its aqueous solubility. According to the available experimental data and considering its dose/solubility ratio (>250 mL at pH = 1.2–6.8), Class II is the one that better represents the characteristics of the drug.

The drug has been provisionally placed in Class IV in the Pediatric BCS.[36] The pediatric drug solubility classification was determined through the pediatric dose number, which is calculated as Dop= M_{0p}/(V_{0p} • C_s), where M_{0p} is the pediatric highest dose strength (in mg), V_{0p} is the water volume taken with a dose (in mL), and C_s is the solubility (in mg mL^{-1}).

Pharmaceutical Formulations

Nifurtimox is effective when treatment is initiated during the acute stage of the infection; however, its effectiveness in treating the chronic stage of infection proved to be highly variable.[102] Different strains of *T. cruzi* display different susceptibilities to the drug, impacting on its effectiveness.[103,104] Despite the toxicity and solubility issues, the diversity of known pharmaceutical formulations of the drug is rather restricted to a handful of alternatives.

The traditional formulation of nifurtimox (Lampit) consists of 30 mg and 120 mg tablets. These should be administered for 3-4 months,[105] cautioning the patient that prolonged treatment may be associated with significant toxicity, which challenges patients' compliance. The drug is seemingly less tolerated by adults during the chronic phase of Chagas disease.

A new, dividable tablet that can be split by hand on the scored lines is also available; it is specially formulated to disperse in water, which can aid in dosing and administration to pediatric patients who may be unable to swallow whole or half tablets.[106]

Slow, medium, and fast release tablet versions have also been used in clinical studies.[107] Aiming to decrease toxicity and side effects González Martin et al. devised polyalkylcyanoacrylate particles as a targeted delivery system for nifurtimox against *Trypanosoma cruzi*.[108] They used an emulsion polymerization process, where different concentrations of nifurtimox, Tween® 20 (a nonionic surfactant agent), and polymers were processed, yielding particles of approximately 200 nm, as determined by scanning electron microscopy and cytometry; they have a 33% drug load and are capable of releasing 65% of the drug within 6 h at pH 7.4, while the release dropped to 20% at pH 1.2.

During *in vitro* studies, the formulation evidenced considerably increased trypanocidal activity against *T. cruzi* epimastigotes, compared with a standard solution of nifurtimox, achieving parasite reduction rates in the range of 87–94%. However, an unexpected activity was found when the parasites were treated with empty nanoparticles, suggesting that their degradation could result in products that are toxic to the parasites,[109] and casting doubts on the validity of this specific approach.

In addition, a recent patent described a multi-particulate sustained-release capsule formulation based on a water-swellable hydrophilic polymer and a binder,[110] with improved efficacy and safety, and sustainable drug release characteristics (< 50% in 8 h and > 70% after 24 h), resulting in a more stable plasmatic profile of nifurtimox.

The group of Lalatsa and Serrano developed self-nanoemulsified drug delivery systems (SNEDDS) capable of producing easily scalable combined formulations of nifurtimox and benznidazole.[111] These facilitate adjustments of the dose and, upon impregnation on mesoporous silica particles, can be easily converted into an oral solid dosage form. The formulation provided enhanced solubilization of both drugs, and combined tablets prepared from SNEDDS loaded on Syloid 3050 silica demonstrated near complete dissolution and efficacy in epimastigotes and amastigotes of *T. cruzi* at the nanomolar level, with acceptable selectivity indexes in acute murine models of Chagas disease.

Metabolism and Disposition

Treatment of humans and laboratory animals with nifurtimox results in a complex chain of reactions that leads to biochemical changes and ultrastructural modifications. Early investigations on rats using [^{35}S]-labeled nifurtimox (dose range, 2.5–25 mg/kg) showed that at 48 h after an oral or intravenous dose of the drug, the animals excreted > 90% of the mark (urine, 34–38%; feces, 56– 58%). Dogs behaved similarly, excreting 75% of the radioactivity at 72 h after an oral or intravenous dose of 10 mg/kg. In humans, it was shown that the active compound has a relatively short time to peak (1-2 h) and a short half-life (2.95 ± 1.19 h).

The drug undergoes significant metabolism; it has an extensive liver first-pass effect and it is subjected to fast elimination. A high percentage of nifurtimox is converted to metabolites and only 0.5% of a single oral dose of nifurtimox was recovered as an unchanged drug in the urine of rats and dogs. TLC of rat urine revealed over 10 spots containing marked excretion products along with an almost undetectable amount of nifurtimox, suggesting that it was almost completely metabolized.[28]

The disposition of nifurtimox has been studied in isolated perfused rat livers, employing a recirculating system.[112] Perfusate samples were analyzed after administration of the drug as bolus (5-30 μg mL^{-1}), observing the monoexponential disappearance of the drug. Nifurtimox was cleared slowly from the rat isolated perfused liver, being poorly extracted by hepatocyte cells and completely metabolized in 2-4 h after perfusion. The elimination constant remained essentially unaltered (0.013 ± 0.002 min^{-1}), the half–life experienced a small increase with the dose (46.6 to 66.8 min), whereas the extraction rate and the distribution volume diminished with the dose (0.128 to 0.099 and 41.1 to 30.7 mL g^{-1}, respectively). The hepatic clearance became halved from the lower to the highest dose (0.66 to 0.34 mL min^{-1} g^{-1}).

The reperfusion of rat livers in recirculation mode with a solution of nifurtimox demonstrated that after a 2 h incubation, nifurtimox became barely detectable, being replaced by highly polar metabolites. Analysis of the perfusate revealed that they retained most of the antiparasitic activity, suggesting the formation of a pharmacologically active metabolite.[26]

Pharmacokinetic studies on nifurtimox in healthy individuals have shown that nifurtimox undergoes extensive metabolism and thus it belongs to class I of the Biopharmaceutic Drug Disposition Classification System (BDDCS).[97] Interestingly, however, in humans with chronic renal failure undergoing hemodialysis the C_{max} is higher due to a change in systemic availability, distribution volume and/or clearance, whereas the mean half-life remained similar to that of healthy subjects.[113]

The mode of action of the drug has been studied, proposing that it is a result of the generation of reactive oxygen species.[114–117] It has also been shown that nifurtimox lowers the intracellular thiol level of *T. cruzi*, and reduction of the nitro moiety with subsequent conjugation to thiols has been proposed as the operating mechanism.[118] The electrochemical study of 5-nitroindazole derivatives using cyclic voltammetry in DMSO provided additional support for this proposal. There, it was evident the generation of nitro-anion radical species, which were characterized by electron spin resonance spectroscopy.[44] On the other hand, molecular orbital calculations, indicated that the LUMO is localized in the NO_2 group.[51]

Among the metabolic enzymes, *T. cruzi* has superoxide dismutase; however, it lacks other enzymes, such as catalase and GSH-peroxidase and it has only low levels of an alternative peroxidase that uses ascorbate.[119] The reduction of nifurtimox to the hydroxylamine and further to the amine can take place under anaerobic conditions. However, it is recognized that the trypanocidal mode of action of nifurtimox is associated with the enzyme-mediated reduction of the drug by the ubiquitous type II nitroreductases, which contain FMN or FAD as a co-factor. They catalyze the one-electron reduction of the substrate with the generation of radicals like $RNO_2^{\bullet}$ (Eq. 4).

Formation of nitroso species (Eq. 5) is also part of the process yielding more reduced derivatives of nifurtimox. In turn, under aerobic conditions the latter can react with oxygen and become involved in a futile cycle to generate the strongly oxidizing species $O_2^{\bullet}$, which is a source of H_2O_2, and regenerate nifurtimox to begin another redox cycle (Eq. 6). In this way, large amounts of $O_2^{\bullet}$ can be produced. The hydronitroxide radical species can also be involved in a similar cycle.[120]

Anaerobic conditions

$$R{-}NO_2 \xrightarrow{+1e^-} R{-}NO_2^{\bullet} \xrightarrow{+1e^-} R{-}NO \xrightarrow{+1e^-} R{-}NHO^{\bullet} \xrightarrow{+1e^-} R{-}NHOH \xrightarrow{+2e^-} R{-}NH_2$$

Nitro-aromatic — **Radical nitroanion** — **Nitroso** — **Hydronitroxide radical** — **Hydroxylamine** — **Amine**

Aerobic conditions

Eq. 4 $2\ R\text{-}NO_2 + NAD(P)H \xrightarrow{\text{Reductase}} 2\ RNO_2^{\bullet} + NAD(P)^+ + H^+$

Eq. 5 $2\ R\text{-}NO_2^{\bullet} + 2\ H^+ \longrightarrow R\text{-}NO_2 + R\text{-}NO + H_2O$

Eq. 6 $R\text{-}NO_2^{\bullet} + O_2 \longrightarrow R\text{-}NO_2 + O_2^{\bullet}$

Eq. 7 $2\ O_2^{\bullet} \xrightarrow{\text{Superoxide dismutase}} O_2^{\bullet} + H_2O_2$

Eq. 8 $O_2^{\bullet} + H_2O_2 \xrightarrow{Fe^{III}} 2\ HO^{\bullet} + O_2$

The $O_2^{\bullet}$ species can undergo dismutation to H_2O_2 and O_2 under SOD catalysis (Eq. 7). On the other hand, H_2O_2 and $O_2^{\bullet}$ can participate in heavy metal catalyzed reactions (Eq. 8), resulting in more toxic radical oxygen species. Such species, like $OH^{\bullet}$ and singlet oxygen ($^1O_2$) can cause permanent DNA damage, enzymatic inhibition, and oxidation of sulfhydryl groups in proteins.

Formation of the radical nitro-anion was detected under anaerobic conditions using electron paramagnetic resonance spectrometry.[121,122] Under these conditions, the radical nitro-anion can undergo subsequent reduction to unstable compounds and stable metabolites depending on the oxygen pressure of the medium and the reaction kinetics,[123] giving rise to more reduced and very toxic forms.

The nitro-anion and nitroxide radicals have been detected as intermediaries[124] and it has been postulated that these reactions proceed sequentially in one-electron reduction stages leading to the nitroso and hydroxylamine en route to the amine derivative.

It has also been shown that nifurtimox reacts with thiol-containing compounds, such as coenzyme A (CoA), lipoic acid (LA), glutathione (GSH), and cysteine (RSH) to produce nitrite (NO_2^-), which is excreted in urine. Using GSH and RSH, it was shown that formation of nitrite was accompanied by the decrease in drug concentration and the formation of a reaction product. This type of reaction might have toxicological relevance, since it may be involved in the side-effects as well as in the chemotherapeutic effects of nifurtimox on *Trypanosoma cruzi*, whereas the reaction with GSH might be key to detoxification of the drug.

In one of the most recent investigations, Lang et al. performed *in vitro* studies on the metabolism of the drug, employing ^{14}C-labeled nifurtimox as substrate along with hepatic and renal sources. They obtained urine, plasma, and fecal rat samples, and also analyzed samples of human urine and plasma by HPLC/HRMS and HRMS/MS with offline liquid scintillation counting for the radiolabeled samples.[125]

The *in vitro* incubations with hepatocytes and subcellular fractions yielded traces of metabolites; in contrast, rat urine enabled the identification of over 30 metabolites. The characteristic MS/MS fragmentation of the metabolites was used to propose structures for 18 metabolites and to synthesize the six most abundant products (Fig. 4) to confirm their structures by HRMS and 2D NMR. It has been shown that typical hepatic and renal drug-metabolizing enzymes are not the main pathway; instead, the drug is rapidly metabolized by reduction, nucleophilic attack, and eventually through oxidation, to a minor extent.

The group of Garcia Bournisan also found the main metabolites of nifurtimox in pediatric urine using a fast tandem MS/MS method.[126] Compounds **31-33** result from furan ring opening and dehydration, whereas **6** is a hydrolysis metabolite. Formation of the pyridone metabolites containing a cysteine residue (**34** and **35**) confirmed previous results on the interaction of nifurtimox with thiol-containing compounds.

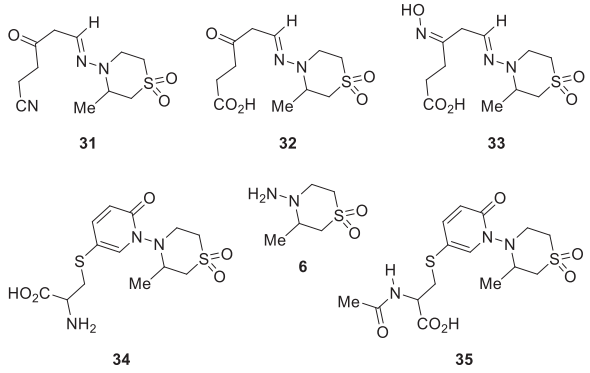

Figure 4. Structures of metabolites of nifurtimox synthesized by Lang et al.[125]

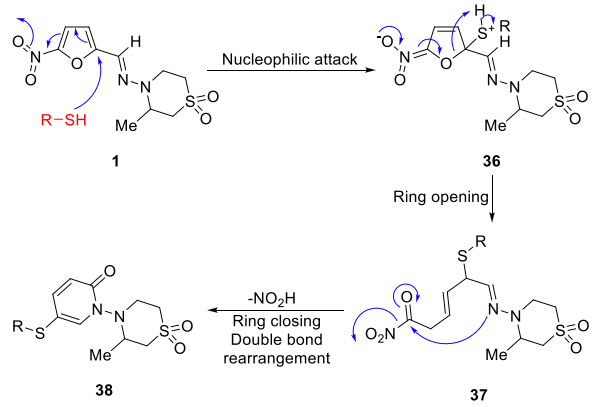

Scheme 10. Proposed mechanism of the formation of 2-pyridone-type metabolites of nifurtimox, by nucleophilic attack of thiols.[125]

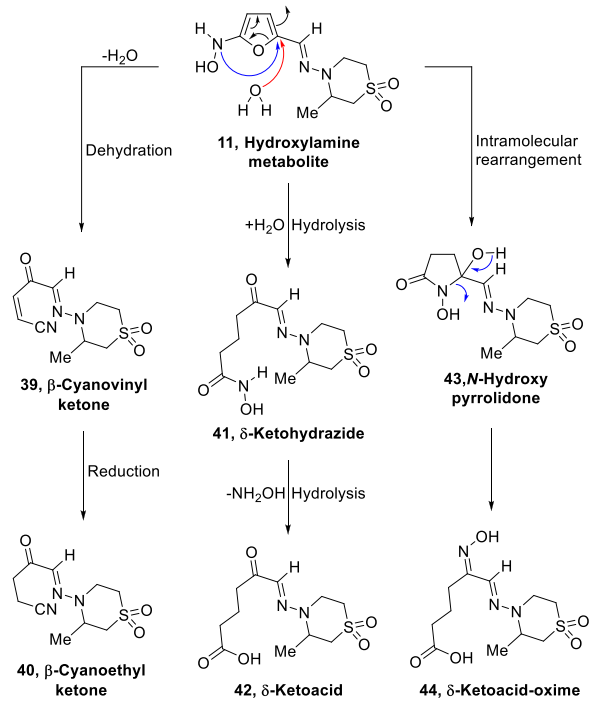

Scheme 11. Proposed mechanism of the formation of nifurtimox metabolites derived from the hydroxylamine **11**.[125]

The mechanism for the formation of such compounds entails a first nucleophilic attack of the thiol to the furan ring of the drug, aided by the nitro moiety (Scheme 10), which results in a ring opening process through intermediate **36**, to afford the α-nitroketone **37**, followed by loss of nitrite ion, and further ring-closing and double bond rearrangement to the pyridone **38**.

It was also shown that the hydroxylamine **11** is a reduction product of nifurtimox, which can undergo additional transformations, namely dehydration, hydrolysis, and intramolecular rearrangement (Scheme 11) to afford additional metabolites. This compound has also been postulated as a precursor of the amine **12**, which is believed to be inert, and of nitrenium species, which can break DNA.[127–130]

The dehydration results in the ring-opened β-cyano enone **39**, which is further reduced to the β-cyanoethylketone **40**. Nitrile derivatives have also been observed in similar compounds,[131,132] and the unsaturated nitrile **39** was observed by HPLC/MS after exposing nifurtimox to the trypanosomal type I nitroreductase TcNTR, being more abundant than its reduced counterpart **40**. Its structure was

confirmed by UV-Vis and tandem MS/MS analyses (ESI+ mode). The unsaturated nitrile **39** proved to inhibit both, parasite and mammalian cell growth at equivalent concentrations.[133] The stability and activity of this compound may explain why nifurtimox is an effective anti-parasitic agent despite being a poor substrate for the nitroreductases.

On the other hand, hydrolysis of the furan ring gives a ring-opened δ-ketohydrazide (**41**), which can undergo additional hydrolysis to the corresponding δ-ketoacid (**42**). In addition, the intramolecular rearrangement resulting from an attack of the hydroxylamine nitrogen on the furan ring results in the unstable *N*-hydroxypyrrolidone intermediate **43**, which suffers ring opening to afford the δ-ketoacid-oxime **44**.

Conclusions

Chagas disease is a parasitic disease caused by *Trypanosoma cruzi*. It is mainly endemic to the Americas, from the Great Lakes of North America to Southern Patagonia, but is spreading to other continents as a result of the migration of infected people. Nifurtimox, a nitrofuran hydrazone derivative, is one of the only two drugs currently available for treating the disease.

Although nifurtimox has been in the market for over 50 years, knowledge of its analytical and pharmaceutical profiles is still fragmentary. This work has collected the most relevant details on the synthesis, characterization and analytical determination of the drug. Spectroscopic, electrochemical and chromatographic methods (including chiral alternatives) for the determination of nifurtimox provide a wide choice depending on the needs of the specific situation. Pharmaceutically important aspects, such as the BCS classification of nifurtimox, its pharmaceutical formulations and metabolism have also been covered, including the identity of the main metabolites.

Considering that nifurtimox is an essential drug, that various efforts for its repurposing in the area of cancer have been made with promising results, that research on the drug is still an active topic, and that the drug is increasingly mentioned in the scientific literature, this review may result in a useful platform for additional discoveries and the development of new knowledge.

Declaration of Competing Interests

The authors declare that they have no known competing financial interests or personal relationships that could have appeared to influence the work reported in this paper.

Acknowledgements

The authors gratefully acknowledge Consejo Nacional de Investigaciones Científicas y Técnicas (CONICET, PUE IQUIR 2016), Agencia Nacional de Promoción Científica y Tecnológica (ANPCyT, PICT 2019-1155) and Agencia Santafesina de Ciencia, Tecnología e Innovación (ASaCTeI, IO-2019-302). ABM is also grateful to CONICET for her doctoral fellowship.

References

1. Rassi Jr A, Rassi A, Little WC. Chagas' heart disease. *Clin Cardiol*. 2000;23:883–889. https://doi.org/10.1002/clc.4960231205.
2. Rocha MOC, Teixeira MM, Ribeiro AL. An update on the management of Chagas cardiomyopathy. *Expert Rev Anti-Infect Ther*. 2007;5:727–743. https://doi.org/10.1586/14787210.5.4.727.
3. Ribeiro AL, Nunes MP, Teixeira MM, Rocha MOC. Diagnosis and management of Chagas disease and cardiomyopathy. *Nat Rev Cardiol*. 2012;9:576–589. https://doi.org/10.1038/nrcardio.2012.109.
4. Martins-Melo FR, Ramos Jr AN, Alencar CH, Heukelbach J. Multiple causes of death related to Chagas' disease in Brazil 1999 to 2007. *J Rev Soc Bras Med Trop*. 2012;45:591–596. https://doi.org/10.1590/S0037-86822012000500010.
5. Perez-Molina JA, Molina I. Chagas disease. *Lancet*. 2018;391(10115):82–94. https://doi.org/10.1016/S0140-6736(17)31612-4.
6. Jannin J, Villa L. An overview of Chagas disease treatment. *Mem Inst Oswaldo Cruz*. 2007;102(Suppl. 1):95–97. https://doi.org/10.1590/s0074-02762007005000106.
7. Priotto G, Fogg C, Balasegaram M, Erphas O, Louga A, Checchi F, Ghabri S, Piola P. Three drug combinations for late-stage Trypanosoma brucei gambiense sleeping sickness: a randomized clinical trial in Uganda. *PLoS Clin Trials*. 2006;1:e39. https://doi.org/10.1371/journal.pctr.0010039.
8. Priotto G, Kasparian S, Mutombo W, Ngouama D, Ghorashian S, Arnold U, Ghabri S, Baudin E, Buard V, Kazadi-Kyanza S, Ilunga M, Mutangala W, Pohlig G, Schmid C, Karunakara U, Torreele E, Kande V. Nifurtimox-eflornithine combination therapy for second-stage African Trypanosoma brucei gambiense trypanosomiasis: a multicentre randomised phase III non-inferiority trial. *Lancet*. 2009;374:56–64. https://doi.org/10.1016/S0140-6736(09)61117-X.
9. Ranjita S. Nanosuspensions: a new approach for organ and cellular targeting in infectious diseases. *J Pharm Invest*. 2013;43:1–26. https://doi.org/10.1007/s40005-013-0051-x.
10. Saulnier Sholler GL, Kalkunte S, Greenlaw C, McCarten K, Forman E. Antitumor activity of nifurtimox observed in a patient with neuroblastoma. *J Pediatr Hematol Oncol*. 2006;28:693–695. https://doi.org/10.1097/01.mph.0000212994.56812.f2.
11. Saulnier Sholler GL, Brard L, Straub JA, Dorf L, Illeyne S, Koto K, Kalkunte S, Bosenberg M, Ashikaga T, Nishi R. Nifurtimox induces apoptosis of neuroblastoma cells in vitro and in vivo. *J Pediatr Hematol Oncol*. 2009;31:187–193. https://doi.org/10.1097/MPH.0b013e3181984d91.
12. Bailly C. Toward a repositioning of the antibacterial drug nifuroxazide for cancer treatment. *Drug Discov Today*. 2019;24:1930–1936. https://doi.org/10.1016/j.drudis.2019.06.017.
13. Saulnier Sholler GL, Swamy N, Kalkunte S, Singh RK, Brard L, Kim KK. *Nitrofuran Compounds for the Treatment of Cancer and Angiogenesis*. 2015. Patent US 9220714.
14. Foces-Foces MC, Cano FH, Claramunt RM, Fruchier A, Elguero J. Molecular structure in the solid state and in solution of nifurtimox and two pyrazol-1-yl analogs. *Bull Soc Chim Belg*. 1988;97:1055–1066. https://doi.org/10.1002/bscb.19880971131.
15. Alarcón de Noya B, Ruiz-Guevara R, Noya O, Castro J, Ossenkopp J, Díaz-Bello Z, Colmenares C, Suárez JA, Noya- Alarcón O, Naranjo L, Gutiérrez H, Quinci G, Torres J. Long-term comparative pharmacovigilance of orally transmitted Chagas disease: first report. *Expert Rev Anti-Infect Ther*. 2017;15:319–325. https://doi.org/10.1080/14787210.2017.1286979.
16. Cancado JR. Long term evaluation of etiological treatment of Chagas disease with benznidazole. *Rev Inst Med Trop Sao Paulo*. 2002;44:29–37. https://doi.org/10.1590/S0036-46652002000100006.
17. Fabbro De Suasnábar D, Arias E, Streiger M, Piacenza M, Ingaramo M, Del Barco M, Amicone N. Evolutive behavior towards cardiomyopathy of treated (nifurtimox or benznidazole) and untreated chronic chagasic patients. *Rev Inst Med Trop Sao Paulo*. 2000;42:99–109. https://doi.org/10.1590/s0036-46652000000200007.
18. Bock M, Haberkorn A, Herlinger H, Mayer KH, Petersen S. The structure-activity relationship of 4-(5′-nitrofurfurylidene-amino)-tetrahydro-4H-14-thiazine-11-dioxides active against Trypanosoma cruzi. *Arzneimittelforschung/Drug Res*. 1972;22:1564–1569.
19. Saulnier Sholler GL, Henna Malini S, Kalkunte S, Singh RK, Laurent B, Kim KK. *Brown University Women & Infants Hospital of Rhode Island). Nitrofuran Compounds for the Treatment of Cancer and Angiogenesis*. 2007. Patent WO2007/108947A2.
20. Heinz H, Heinrich MK, Bayer AG. *Production of Substituted Tetrahydro-14-Thiazine-11-Dioxides*. 1970. Patent US3541090.
21. Romdhani-Younes M, Chaabouni MM. Efficient synthesis of ββ′-dihydroxy sulfides by ring opening of epoxides with mercaptoethanol catalyzed under solvent-free conditions. *J Sulfur Chem*. 2012;33:223–228. https://doi.org/10.1080/17415993.2012.662685.
22. Brard L, Singh RK, Kim KK, Saulnier-Sholler G. *(Brown University Women & Infants Hospital of Rhode Island). N-Amino Tetrahydrothiazine Derivatives Method of Manufacture and Use*. 2008. Patent WO2008091946.
23. Herlinger H, Mayer K-H, Petersen S, Bock M, Bayer AG. *Novel 5-Nitro-Furfurylidene-(2) Derivatives and Process for Producing the Same*. 1964. Patent DE1170957.
24. Giller SA, Venter KK, Trushule MA, Berggrin GE, Brinkmanis RA, Mikstais UY, Stankevich PA. Method of preparing 5-nitrofurfural diacetate. *Patent US4052419A1*. 1977.
25. Trant JF, Meister D, Nasri S, Chifor AE, Hayward J, Taimoory SM, Dashti-Pour M. *(University of Windsor). Thermally Sensitive Protecting Groups for Cysteine and Manufacture and Use Thereof*. 2021. Patent US 2021/0040105.
26. Gonzalez-Martin G, Paulos C, Guevara A, Ponce G. Disposition of nifurtimox and metabolite activity against Trypanosoma cruzi using rat isolated perfused liver. *J Pharm Pharmacol*. 1994;46:356–359. https://doi.org/10.1111/j.2042-7158.1994.tb03812.x.
27. Jeganathan S, Sanderson L, Dogruel M, Rodgers J, Croft S, Thomas SA. The distribution of nifurtimox across the healthy and trypanosome-infected murine blood-brain and blood-cerebrospinal fluid barriers. *J Pharmacol Exp Ther*. 2011;336:506–515. https://doi.org/10.1124/jpet.110.172981.
28. Duhm B, Maul W, Medenwald H, Patzschke K, Wegner LA. Investigations on the pharmacokinetics of nifurtimox-^{35}S in the rat and dog. *Arzneimittelforschung/Drug Res*. 1972;22:1617–1624.

29. Mester B, Elguero J, Claramunt RM, Castanys S, Mascaro ML, Osuna A, Vilaplana MA, Molina P. Activity against Trypanosoma cruzi of new analogues of nifurtimox. *Arch Pharm*. 1987;320:115–120. https://doi.org/10.1002/ardp.19873200205.
30. Asinger F, Saus A, von Wachtendonk M. Zur Kenntnis der Reaktionsfähigkeit des Thiomorpholins und alkylsubstituierter Thiomorpholine 4. Mitt. *Monatsh. Chem*. 1980;111:385–398. https://doi.org/10.1007/BF00903234.
31. Popp FD. Potential anticonvulsants. XII. Anticonvulsant activity of some aldehyde derivatives. *Eur J Med Chem*. 1989;24:313–316. https://doi.org/10.1016/0223-5234(89)90016-0.
32. Enders D, Braig V, Boudou M, Raabe G. Asymmetric synthesis of 3-substituted dihydro-2H-isoquinolin-1-ones dihydro and tetrahydroisoquinolines via 12-addition/ring closure. *Synthesis*. 2004:2980–2990. https://doi.org/10.1055/s-2004-834861.
33. Filali-Mouhim A, Champion B, Jore D, Hickel B, Ferradini C. Réduction radiolytique du nifurtimox par les radicaux libres. *J Chim Phys Phys*. 1991;88:937–943. https://doi.org/10.1051/jcp/1991880937.
34. Sreedhar NY, Jayarama Reddy S. Electrochemical behaviour of nitrofuran. *J Indian Chem Soc*. 1991;68:562–566.
35. Moraes CB, White KL, Braillard S, Perez C, Goo J, Gaspar L, Shackleford DM, Cordeiro-da-Silva A, Thompson RCA, Freitas Jr L, Charman SA, Chatelain E. Enantiomers of nifurtimox do not exhibit stereoselective anti-trypanosoma cruzi activity toxicity or pharmacokinetic properties. *Antimicrob Agents Chemother*. 2015;59:3645–3647. https://doi.org/10.1128/AAC.05139-14.
36. del Moral Sanchez JM, Gonzalez-Alvarez I, Cerda-Revert A, Gonzalez-Alvarez M, Navarro-Ruiz A, Amidon GL, Bermejo M. Biopharmaceutical optimization in neglected diseases for paediatric patients by applying the provisional paediatric biopharmaceutical classification system. *Br J Clin Pharmacol*. 2018;84:2231–2241. https://doi.org/10.1111/bcp.13650.
37. Roth L, Adler M, Jaina T, Bempong D. Monographs for medicines on WHO's model list of essential medicines. *Bull World Health Org*. 2018;96:378–385. https://doi.org/10.2471/BLT.17.205807.
38. Alves MA, de Queiroz AC, Alexandre-Moreira MS, Varela J, Cerecetto H, González M, Doriguetto AC, Landre IM, Barreiro EJ, Lima LM. *Eur J Med Chem*. 2015;100:24–33. https://doi.org/10.1016/j.ejmech.2015.05.046.
39. Palace-Berl F, Pasqualoto KFM, Zingales B, Moraes CB, Bury M, Franco CH, Lopes da Silva Neto A, Murayama JS, Nunes SL, Nunes Silva M, Costa Tavares L. Investigating the structure-activity relationships of N'-(5-nitrofuran-2-yl) methylene. substituted hydrazides against Trypanosoma cruzi to design novel active compounds. *Eur J Med Chem*. 2018;144:29–40. https://doi.org/10.1016/j.ejmech.2017.12.011.
40. Álvarez G, Perdomo C, Coronel C, Aguilera E, Varela J, Aparicio G, Zolessi FR, Cabrera N, Vega C, Rolón M, Rojas de Arias A, Pérez-Montfort E, Cerecetto H, González M. Multi-anti-parasitic activity of arylidene ketones and thiazolidene hydrazines against Trypanosoma cruzi and Leishmania spp. *Molecules*. 2017;22: 709. https://doi.org/10.3390/molecules22050709.
41. Núñez-Vergara LJ, Aldunate J, Letelier ME, Bollo S, Repetto Y, Morello A, Spencer PL, Squella JA. Nitro radical anion formation from nifurtimox II: electrochemical evidence. *Bioelectrochem Bioenerg*. 1995;38:355–358. https://doi.org/10.1016/0302-4598(95)05023-2.
42. Bautista-Martinez JA, González I, Aguilar-Martínez M. Influence of the acidity level change in aprotic media on the voltammetric behavior of nitrogabacinamamides. *Electrochim Acta*. 2004;49:3403–3411. https://doi.org/10.1016/j.electacta.2004.03.008.
43. Sánchez-Urbán DG, Díaz de León-Luna P, Bautista-Martínez JA, Frontana C, González I, Aguilar-Martínez M. Interaction of antiprotozoal drugs with biomolecules. An ESR and UV-vis spectroelectrochemical study. *ECS Trans*. 2007;3:167–174.
44. Folch-Cano C, Olea-Azara C, Arán VJ, Diaz-Urrutia C. ESR and electrochemical study of 12-disubstituted 5-nitroindazolin-3-ones and 2-substituted 3-alkoxy-5-nitro-2H-indazoles: Reactivity and free radical production capacity in the presence of biological systems. *Spectrochim Acta A*. 2010;75:375–380. https://doi.org/10.1016/j.saa.2009.10.044.
45. Otero L, Vieites M, Boiani L, Denicola A, Rigol C, Opazo L, Olea-Azar C, Maya JD, Morello A, Krauth-Siegel RL, Piro OE, Castellano E, González M, Gambino D, Cerecetto H. Novel antitrypanosomal agents based on palladium nitrofuryl thiosemicarbazone complexes: DNA and redox metabolism as potential therapeutic targets. *J Med Chem*. 2006;49:3322–3331. https://doi.org/10.1021/jm0512241.
46. Vieites M, Otero L, Santos D, Toloza J, Figueroa R, Norambuena E, Olea-Azar C, Aguirre G, Cerecetto H, González M, Morello A, Maya JD, Garat B, Gambino D. Platinum(II) metal complexes as potential anti-Trypanosoma cruzi agents. *J Inorg Biochem*. 2008;102:1033–1043. https://doi.org/10.1016/j.jinorgbio.2007.12.005.
47. Olea-Azar C, Atria AM, di Maio R, Seoane G, Cerecetto H. Electron spin resonance and cyclic voltammetry studies of nitrofurane and nitrothiophene analogues of nifurtimox. *Spectrosc Lett*. 1988;31:849–857. https://doi.org/10.1080/00387019808007403.
48. Bollo S, Núñez-Vergara LJ, Bonta M, Chauviere G, Périé J, Squella JA. Cyclic voltammetric studies on nitro radical anion formation from megazol and some related nitroimidazole derivatives. *J Electroanal Chem*. 2011;511:46–54. https://doi.org/10.1016/S0022-0728(01)00557-5.
49. Viodé C, Bettache N, Cenas N, Krauth-Siegel RL, Chauviere G, Bakalara N, Périé J. Enzymatic reduction studies of nitroheterocycles. *Biochem Pharmacol*. 1999;57:549–557. https://doi.org/10.1016/s0006-2952(98)00324-4.
50. Olea-Azar C, Atria AM, Mendizabal F, di Maio R, Seoane G, Cerecetto H. Cyclic voltammetry and electron paramagnetic resonance studies of some analogues of nifurtimox. *Spectrosc Lett*. 1998;31:99–109. https://doi.org/10.1080/00387019808006764.
51. Echeverría C, Romero V, Arancibia R, Klahn H, Montorfano I, Armisen R, Borgna V, Simon F, Ramirez-Tagle R. The characterization of anti-T. cruzi activity relationships between ferrocenyl cyrhetrenyl complexes and ROS release. *BioMetals*. 2016;29:743–749. https://doi.org/10.1007/s10534-016-9953-1.
52. Chaves OA, Ferreira RC, da Silva LS, de Souza BCE, Cesarin-Sobrinho D, Netto-Ferreira JC, Sant'Anna CMR, Ferreira ABB. Multiple spectroscopic and theoretical approaches to study the interaction between HSA and the antiparasitic drugs: benznidazole, metronidazole, nifurtimox and megazol. *J Braz Chem Soc*. 2018;29:1551–1562. https://doi.org/10.21577/0103-5053.20180029.
53. Holzer W. Determination of the stereochemistry of chemotherapeutics derived from 5-nitrofurfural: NOE difference spectroscopy as a simple and reliable method. *Arch. Pharm*. 1992;25:769–772. https://doi.org/10.1002/ardp.19923251205.
54. Popelis YY, Liepin'sh EE, Stradyn YP. ^{1}H and ^{13}C NMR spectra of 2-substituted 5-nitrofurans and conformation of chemotherapeutic preparations of the 5-nitrofuran series. *Chem Heterocyclic Comp USSR*. 1980;16:116–123. https://doi.org/10.1007/BF02401683.
55. Bird CW. Cheeseman GWH. In: Katritzky AR, Rees CW, eds. *Comprehensive Heterocyclic Chemistry*. Pergamon Press Oxford; 1984:33. vol. 4 and references therein.
56. Moroni AB, Pérez Mayoral E, Lionello DF, Vega DR, Kaufman TS, Calvo NL. Solid-state properties of Nifurtimox. Preparation characterization and stability of an amorphous phase. *Eur J Pharm Biopharm*. 2023;184:25–35. https://doi.org/10.1016/j.ejpb.2023.01.008.
57. Squella JA, Muñoz W, Paulos C, Nunez-Vergara LJ. Polarographic study of Nifurtimox. *J. Pharm. Sci*. 1990;79:837–839. https://doi.org/10.1002/jps.2600790920.
58. Medenwald H, Brandau K, Schlossmann K. Quantitative determination of nifurtimox in body fluids of rat dog and man. *Arzneimittelforschung*. 1972;22:1613–1616.
59. Bulffer RF, Castro JA, Fanelli SL. UV methodology for determination of antichagasic drugs Nifurtimox and Benznidazole in blood. *Acta Bioquím Clín Latinoam*. 2011;45:463–470.
60. Sastry CSP, Rama Rao K, Murali Krishna D, Sastry BS, Siva Prasad D. Spectrophotometric methods for the determination of nifurtimox in bulk form and pharmaceutical formulations. *Talanta*. 1994;41:1957–1963. https://doi.org/10.1016/0039-9140(94)00155-3.
61. Fabregas JL, Casassas E. Spectrophotometric determination of nitrofurazone with phloroglucinol. *Anal Chim Acta*. 1979;107:401–404. https://doi.org/10.1016/S0003-2670(01)93236-2.
62. Sawicki E, Stanley TW, Hauser TR, Elbert W, Noe JL. The 3-methyl-2-benzothiazolone hydrazone test. Sensitive new methods for the detection rapid estimation and determination of aliphatic aldehydes. *Anal Chem*. 1961;33:93–96. https://doi.org/10.1021/ac60169a028.
63. Pays M, Bourdon R, Beljean M. Diazo coupling of amines and nitrogenous heterocyclic compounds using the HMBT reaction. *Anal Chim Acta*. 1969;47:101–111. https://doi.org/10.1016/s0003-2670(01)81809-2.
64. Hassan SM, Sharaf El-Din M, Bela F, Sultan M. Spectrophotometric determination of some pharmaceutically important nitro compounds in their dosage forms. *Analyst*. 1988;113:1087–1089. https://doi.org/10.1039/AN9881301087.
65. Hassan SM, Sharaf El-Din M, Bela F, Sultan M. Application of difference spectroscopy to the determination of some pharmaceutically important nitro compounds. *J Pharm Pharmacol*. 1988;40:798–800. https://doi.org/10.1111/j.2042-7158.1988.tb05175.x.
66. Brownley Jr. AC, L Lachman. Browning of spray-processed lactose. *J Pharm Sci*. 1964;3:452–454. https://doi.org/10.1002/jps.2600530428.
67. Sastry CSP, Reddy BS, Rao BG. Spectrophotometric determination of some antitubercular drugs. *Indian J Pharm Sci*. 1981;43:118–120.
68. Sastry CSP, Srinivas KR, Krishna Prasad KMM. Spectrophotometric determination of drugs in pharmaceutical formulations withN-bromosuccinimide and celestine blue. *Mikrochim Acta*. 1996;122:77–86. https://doi.org/10.1007/BF01252408.
69. Sastry CSP, Rama Srinivas K, Krishna Prasad KMM. Spectrophotometric determination of bio-active compounds with chloramine-T and gallocyanine. *Talanta*. 1996;43:1625–1632. https://doi.org/10.1016/0039-9140(96)01862-0.
70. Paulos C, Paredes J, Vasquez I, Kunze G, Gonzalez-Martin G. HPLC determination of nifurtimox in human serum. *J Chromatogr*. 1988;433:359–362. https://doi.org/10.1016/S0378-4347(00)80621-0.
71. Gnoth M-J, Hopfe PM, Thuss U. Determination of nifurtimox in dog plasma by stable-isotope dilution LC-MS/MS. *Bioanalysis*. 2015;7:2777–2787. https://doi.org/10.4155/bio.15.185.
72. Montalto de Mecca M, Diaz EG, Castro JA. Nifurtimox biotransformation to reactive metabolites or nitrite in liver subcellular fractions and model systems. *Toxicol Lett*. 2002;136:1–8. https://doi.org/10.1016/s0378-4274(02)00238-2.
73. Díaz EG, Montalto de Mecca M, Castro JA. Reactions of nifurtimox with critical thiol-containing biomolecules. Their potential toxicological relevance. *J Appl Toxicol*. 2004;24:189–195. https://doi.org/10.1002/jat.970.
74. Padro JM, Marson ME, Mastrantonio GE, Altcheh J, Garcia-Bournissen F, Reta M. Development of an ionic liquid-based dispersive liquid-liquid microextraction method for the determination of nifurtimox and benznidazole in human plasma. *Talanta*. 2013;107:95–102. https://doi.org/10.1016/j.talanta.2012.12.050.
75. Padro JM, Pellegrino Vidal RB, Echevarria RN, Califano AN, Reta MR. Development of an ionic-liquid-based dispersive liquid-liquid microextraction method for the determination of antichagasic drugs in human breast milk: optimization by central composite design. *J Sep Sci*. 2015;38:1591–1600. https://doi.org/10.1002/jssc.201401367.

76. Moroni S, Marson ME, Moscatelli G, Mastrantonio G, Bisio M, Gonzalez N, Ballering G, Altcheh J, Garcia-Bournissen F. Negligible exposure to nifurtimox through breast milk during maternal treatment for Chagas Disease. *PLOS Negl Trop Dis*. 2019;13: e0007647. https://doi.org/10.1371/journal.pntd.0007647.
77. Chankvetadze B, Kartozia I, Yamamoto C, Okamoto Y. Comparative enantioseparation of selected chiral drugs on four different polysaccharide-type chiral stationary phases using polar organic mobile phases. *J Pharm Biomed Anal*. 2002;27:467–478. https://doi.org/10.1016/S0731-7085(01)00648-3.
78. Chankvetadze L, Kartozia I, Yamamoto C, Chankvetadze B, Blaschke G, Okamoto Y. Enantioseparations in nonaqueous capillary liquid chromatography and capillary electrochromatography using cellulose tris(35-dimethylphenylcarbamate) as chiral stationary phase. *Electrophoresis*. 2002;23:486–493. https://doi.org/10.1002/1522-2683(200202)23:3<486::AID-ELPS486>3.0.CO;2-L.
79. Lipinski CA. Lead- and drug-like compounds: the rule-of-five revolution. *Drug Discov Today*. 2004;1:337–341. https://doi.org/10.1016/j.ddtec.2004.11.007.
80. From: https://www.labnetwork.com/frontend-app/p/#!/moleculedetails/LN01374879 (Accessed 10 February 2023).
81. Veber DF, Johnson SR, Cheng H-Y, Smith BR, Ward KW, Kopple KD. Molecular properties that influence the oral bioavailability of drug candidates. *J Med Chem*. 2002;45:2615–2623. https://doi.org/10.1021/jm020017n.
82. *World Health Organization. The International Pharmacopoeia*. 10th Ed. 2020. Available at; https://digicollections.net/phint/2020/index.html#d/b.6.1.252. (Accessed 13 January 2023).
83. Earley JV, Ma TS. Titanous chloride as a reagent for quantitative organic micro analysis. II. Microdetermination of azo and diazonium compounds and of nitro arylhydrazines. *Microchim Acta*. 1960;48:685–692. https://doi.org/10.1007/BF01216052.
84. Park KY, Choi MG, Lee YJ, Chang S-K. Colorimetric and fluorogenic determination of Ti^{3+} ions via nitro-to-amine conversion of nitronaphthalimides. *Sens Actuat B*. 2019;282:684–689. https://doi.org/10.1016/j.snb.2018.11.082.
85. Amidon GL, Lennernäs H, Shah VP, Crison JR. A theoretical basis for a biopharmaceutic drug classification: the correlation of in vitro drug product dissolution and in vivo bioavailability. *Pharm Res*. 1995;12:413–420. https://doi.org/10.1208/s12248-014-9620-9.
86. Lindenberg M, Kopp S, Dressman JB. Classification of orally administered drugs on the World Health Organization Model list of Essential Medicines according to the biopharmaceutics classification system. *Eur J Pharm Biopharm*. 2004;58:265–278. https://doi.org/10.1016/j.ejpb.2004.03.001.
87. Dahan A, Wolk O, Kim YH, Ramachandran C, Crippen GM, Takagi T, Bermejo M, Amidon GL. Purely in silico BCS classification: science based quality standards for the world's drugs. *Mol Pharm*. 2013;10:4378–4390. https://doi.org/10.1021/mp400485k.
88. Oliveira M, Dias A, Pontes V, Souza Jr A, Coelho H, Coelho I. A critical review on Chagas disease chemotherapy. *Mem Inst Oswaldo Cruz*. 2002;97:3–24. https://doi.org/10.1590/s0074-02762002000100001.
89. Oliveira M, Dias A, Pontes V, Souza Jr A, Coelho H, Coelho I. Tratamento etiológico da doença de Chagas no Brasil. *Rev Patol Trop*. 2008;37:209–228. https://doi.org/10.5216/rpt.v37i3.5063.
90. Castro JA, de Mecca MM, Bartel LC. Toxic side effects of drugs used to treat Chagas' disease (American trypanosomiasis). *Hum Exp Toxicol*. 2006;25:471–479. https://doi.org/10.1191/0960327106het653oa.
91. Coura J, de Abreu L, Willcox H, Petana W. Efficacy of nifurtimox for the treatment of chronic Chagas disease. *Rev Soc Bras Med Trop*. 1997;30:139–144. https://doi.org/10.4067/S0716-10182012000100013.
92. Kasim NA, Whitehouse M, Ramachandran C, Bermejo M, Lennernäs H, Hussain AS, Junginger HE, Stavchansky SA, Midha KK, Shah VP, Amidon GL. Molecular properties of WHO essential drugs and provisional biopharmaceutical classification. *Mol Pharm*. 2004;1:85–96. https://doi.org/10.1021/mp034006h.
93. Chemicalize by ChemAxon. Available at https://chemicalize.com/#/calculation. (Accessed 13 January 2023).
94. Dave RA, Morris ME. Novel high/low solubility classification methods for new molecular entities. *Int J Pharm*. 2016;511:111–126. https://doi.org/10.1016/j.ijpharm.2016.06.060.
95. Leverkusen Bayer AG. *Stable Tablet Formulation of Nifurtimox and Process for Producing the Same*. 2020. Patent EP 3 750 527 A1.
96. Bennett-Lenane H, Griffin BT, O'Shea JP. Machine learning methods for prediction of food effects on bioavailability: A comparison of support vector machines and artificial neural networks. *Eur J Pharm Sci*. 2022;168: 106018. https://doi.org/10.1016/j.ejps.2021.106018.
97. Paulos C, Paredes J, Vasquez I, Thambo S, Arancibia A, Gonzalez-Martin G. Pharmacokinetics of a nitrofuran compound nifurtimox in healthy volunteers. *Int J Clin Pharmacol Ther Toxicol*. 1989;27:454–457.
98. Sweetman SC. *Martindale 33; Martindale The Extra Pharmacopoeia*. London, UK: Council of the Royal Pharmaceutical Society of Great Britain; 2002.
99. Pham-The H, Garrigues T, Bermejo M, González-Álvarez I, Cruz Monteagudo M, Cabrera-Pérez MA. Molecular properties of WHO essential drugs and provisional biopharmaceutical classification. *Mol Pharm*. 2004;1:85–96. https://doi.org/10.1021/mp034006h.
100. Bergström CAS, Andersson SBE, Fagerberg JH, Ragnarsson G, Lindahl A. Is the full potential of the biopharmaceutics classification system reached? *Eur J Pharm Sci*. 2014;57:224–231. https://doi.org/10.1016/j.ejps.2013.09.010.
101. Khandelwal A, Bahadduri PM, Chang C, Polli JE, Swaan S, Ekins PW. Computational models to assign biopharmaceutics drug disposition classification from molecular structure. *Pharm Res*. 2007;24:2249–2262. https://doi.org/10.1007/s11095-007-9435-9.
102. Coura JR. Chagas disease: what is known and what is needed - a background article. *Mem Inst Oswaldo Cruz*. 2009;104:549–554. https://doi.org/10.1590/s0074-02762009000400002.
103. Filardi LS, Brener Z. Susceptibility and natural resistance of Trypanosoma cruzi strains to drugs used clinically in Chagas disease. *Trans R Soc Trop Med Hyg*. 1987;81:755–759. https://doi.org/10.1016/0035-9203(87)90020-4.
104. Murta SMF, Gazzinelli RT, Brener Z, Romanha A. Molecular characterization of susceptible and naturally resistant strains of Trypanosoma cruzi to benznidazole and nifurtimox. *J Mol Biochem Parasitol*. 1998;93:203–214. https://doi.org/10.1016/s0166-6851(98)00037-1.
105. Chirac P, Torreele E. Global framework on essential health R&D. *Lancet*. 2006;367:1560–1561. https://doi.org/10.1016/S0140-6736(06)68672-8.
106. *Lampit (nifurtimox) Tablets Highlights of Prescribing Information*. Food and Drug Administration (FDA); 2020. https://www.accessdata.fda.gov/drugsatfda_docs/label/2020/213464s000lbl.pdf. (Accessed 13 January 2023).
107. Ince I, Prins K, Willmann S, Sutter G, Hanze E, Sadre-Marandi F, Stass H, Garmann D. Population pharmacokinetics of nifurtimox in adult and pediatric patients with Chagas disease. *J Clin Pharmacol*. 2022;62:1273–1284. https://doi.org/10.1002/jcph.2064.
108. Gonzalez-Martin G, Merino I. Characterization and trypanocidal activity of nifurtimox-containing and empty nanoparticles of polyethylcyanoacrylates. *J Pharm Pharmacol*. 1998;50:29–35. https://doi.org/10.1111/j.2042-7158.1998.tb03301.x.
109. Sánchez G, Cuellar D, Zulantay I, Gajardo M, González-Martin G. Cytotoxicity and trypanocidal activity of nifurtimox encapsulated in ethylcyanoacrylate nanoparticles. *Biol Res*. 2002;35:39. https://doi.org/10.4067/S0716-97602002000100007.
110. Chen D, Rice G, Metronom X. *Novel Formulations of Nitrofurans Including Nifurtimox with Enhanced Activity with Lower Toxicity*. 2015. Patent US 20150140089A1.
111. Rolon M, Hanna E, Vega C, Coronel C, Dea-Ayuela MA, Serrano DR, Lalatsa A. Solid nanomedicines of nifurtimox and benznidazole for the oral treatment of chagas disease. *Pharmaceutics*. 2022;14:1822. https://doi.org/10.3390/pharmaceutics14091822.
112. González-Martin G, Ponce G, Inostroza V, González M, Paulos C, Guevara A. The disposition of nifurtimox in the rat isolated perfused liver: effect of dose size. *J Pharm Pharmacol*. 1993;45:72–74. https://doi.org/10.1111/j.2042-7158.1993.tb03684.x.
113. González-Martin G, Thambo S, Paulos C, Vásquez I, Paredes J. The pharmacokinetics of nifurtimox in chronic renal failure. *Eur J Clin Pharmacol*. 1992;42:671–673. https://doi.org/10.1007/BF00265935.
114. Sreider C, Grinblat L, Stoppani AOM. Catalysis of nitro-furan redox-cycling and superoxide anion production by heart lipoamide dehydrogenase. *Biochem Pharm*. 1990;40:1849–1857. https://doi.org/10.1016/0006-2952(90)90366-S.
115. Maya J, Repetto Y, Agosin M, Ojeda JM, Tellez R, Gaule C, Morello A. Effects of Nifurtimox and Benznidazole upon glutathione and trypanothione in epimastigote trypomastigote and amastigote forms of Trypanosoma cruzi. *Mol Biochem Parasitol*. 1997;86:101–106. https://doi.org/10.1016/S0166-6851(96)02837-X.
116. Docampo R. Sensitivity of parasites to free radical damage by antiparasitic drugs. *Chem-Biol Interact*. 1990;73:1–27. https://doi.org/10.1016/0009-2797(90)90106-w.
117. Docampo R, Stoppani AOM. Generation of superoxide anion and hydrogen peroxide induced by nifurtimox in Trypanosoma cruzi. *Arch Biochem Biophys*. 1979;197:317–321. https://doi.org/10.1016/0003-9861(79)90251-0.
118. Blumenstiel K, Schöneck R, Yardley V, Croft SL, Krauth-Siegel RL. Nitrofuran drugs as common subversive substrates of Trypanosoma cruzi lipoamide dehydrogenase and trypanothione reductase. *Biochem Pharmacol*. 1999;58:1791–1799. https://doi.org/10.1016/s0006-2952(99)00264-6.
119. Docampo R, Moreno SNJ. Biochemical toxicology of antiparasitic compounds used in the chemotheraphy and chemoprophylaxis of American Trypanosomiasis (Chagas' disease). *Rev Biochem Toxicol*. 1985;7:159–204.
120. Castro JA. *Ciencia Investigación*. 2014;64(5):78–92.
121. Docampo R, Mason RP, Monley C, Muñiz RPA. Generation of free radicals induced by nifurtimox in mammalian tissues. *J Biol Chem*. 1981;256:10930–10933. https://doi.org/10.1016/S0021-9258(19)68534-0.
122. Femández Villamil SH, Dubín M, Brusa MA, Durán RP, Perissinotti LJ, Stoppani AOM. Generation of radical anions of nifurtimox and related nitrofuran compounds by ascorbate. *Free Rad Res Comm*. 1990;10:351–360. https://doi.org/10.3109/10715769009149904.
123. Holtman JL, Crankshaw DL, Peterson FJ, Polnaszek CF. The kinetics of the aerobic reduction of nitrofurantoin by NADPH-cytochrome P-450 Ic) reductase. *Mol Pharmacol*. 1981;20:669–673.
124. Mason RP, Holtzman JL. The mechanism of microsomal and mitochondrial nitroreductase. Electron spin resonance evidence for nitroaromatic free radical intermediates. *Biochemistry*. 1975;14:1626–1632. https://doi.org/10.1021/bi00679a013.
125. Lang D, Schulz SI, Piel I, Tshitenge DT, Stass H. Structural and mechanistic investigation of the unusual metabolism of nifurtimox. *Chem Res Toxicol*. 2022;35:2037–2048. https://doi.org/10.1021/acs.chemrestox.2c00210.
126. Pérez Montilla CA, Moroni S, González N, Moscatelli G, Altcheh JM. García Bournissen F. Identification of nifurtimox metabolites in urine of pediatric Chagas disease patients by UHPLC-MS/MS. *Arch Dis Child*. 2019;104:e32–e33. https://doi.org/10.1136/archdischild-2019-esdppp.76.
127. Swaminathan S, Jr Lower GM, Bryan GT. Nitroreductase-mediated metabolic activation of 2-amino-4-(5-nitro-2-furyl)thiazole and binding to nucleic acids and proteins. *Cancer Res*. 1982;42:4479–4484.

128. McCalla DR, Reuvers A, Kaiser C. Breakage of bacterial DNA by nitrofuran derivatives. *Cancer Res*. 1971;31:2184–2188.
129. Streeter AJ, Hoener BA. Evidence for the involvement of a nitrenium ion in the covalent binding of nitrofurazone to DNA. *Pharm Res*. 1988;5:434–436. https://doi.org/10.1023/a:1015988401601.
130. Beckett AH, Robinson AE. The reaction of nitrofurans with bacteria—III. Reduction of a series of antibacterial nitrofurans (type B compounds) by Aerobacter aerogenes. *J Med Pharm Chem*. 1959;1:155–164. https://doi.org/10.1021/jm50003a003.
131. Gavin JJ, Ebetino FF, Freedman R, Waterbury WE. The aerobic degradation of 1-(5-nitrofurfurylideneamino)-2-imidazolidinone (NF-246) by Escherichia coli. *Arch Biochem Biophys*. 1996;13:399–404. https://doi.org/10.1016/0003-9861(66)90205-0.
132. Swaminathan S, Bryan GT. Biotransformation of the bladder carcinogen N-4-(5-nitro-2-furyl)-2-thiazolyl.formamide in mice. *Cancer Res*. 1984;44:2331–2338.
133. Hall BS, Bot C, Wilkinson SR. Nifurtimox activation by trypanosomal type I nitroreductases generates cytotoxic nitrile metabolites. *J Biol Chem*. 2011;286:13088–13095. https://doi.org/10.1074/jbc.M111.230847.